J. Math. Biol. (2012) 65:201–236
DOI 10.1007/s00285-011-0457-x

Mathematical Biology

Evolution of host resistance to parasite infection in the snail–schistosome–human system

Yiding Yang · Zhilan Feng · Dashun Xu · Gregory J. Sandland · Dennis J. Minchella

Received: 7 September 2010 / Revised: 25 March 2011 / Published online: 20 July 2011

Abstract The evolutionary strategies that emerge within populations can be dictated by numerous factors, including interactions with other species. In this paper, we explore the consequences of such a scenario using a host–parasite system of human concern. By analyzing the dynamical behaviors of a mathematical model we investigate the evolutionary outcomes resulting from interactions between *Schistosoma mansoni* and its snail and human hosts. The model includes two types of snail hosts representing resident and mutant types. Using this approach, we focus on establishing evolutionary stable strategies under conditions where snail hosts express different life-histories and when drug treatment is applied to an age-structured population of human hosts. Results from this work demonstrate that the evolutionary trajectories of host–parasite interactions can be varied, and at times, counter-intuitive, based on parasite virulence, host resistance, and drug treatment.

Keywords Host–parasite dynamics · Schistosomiasis · Invasion · Evolutionary stable strategy

Mathematics Subject Classification (2000) 35B40 · 37N25 · 92B05 · 92D30 · 92D40

Y. Yang · Z. Feng (✉)
Department of Mathematics, Purdue University, West Lafayette, IN 47907, USA
e-mail: zfeng@math.purdue.edu

D. Xu
Department of Mathematics, Southern Illinois University Carbondale, Carbondale, IL 62901, USA

G. J. Sandland
Department of Biology, University of Wisconsin–La Crosse, La Crosse, WI 54601, USA

D. J. Minchella
Department of Biological Sciences, Purdue University, West Lafayette, IN 47907, USA

1 Introduction

Studying particular host–parasite interactions can often provide valuable insights into general patterns of disease establishment and persistence in natural systems. Addressing these systems using mathematical models not only provides us with information about the importance of particular disease parameters, but also allows us to follow the outcomes of such interactions over evolutionary time. Currently, most coevolutionary models of host–parasite interactions involve microparasites with direct life cycles (e.g., Anderson and May 1982, 1991; Boots and Bowers 1999; Boots and Haraguchi 1999; Bowers et al. 1994; Frank 1992; May and Anderson 1983; May and Nowak 1995; Miller et al. 2005; Nowak and May 1994). There have been few theoretical studies investigating host–parasite coevolution using indirectly transmitted parasites (e.g., Dobson 1988; Dobson and Keymer 1985). Indirect life cycles involve multiple species of hosts (definitive and intermediate), all of which are required for the parasite to complete its development from larvae to an adult. Variable selective forces imposed by different host species (or strains) can have important consequences for parasite fitness at a number of points throughout the life cycle (see Davies et al. 2001; Gower and Webster 2004, 2005).

Empirical work has demonstrated that parasites may face different host strategies for mitigating or preventing infection at different points in the life cycle (Minchella 1985). In some cases, hosts may actively resist parasite attack by altering morphological, physiological, or immunological factors (Sandland and Minchella 2003a). However, these strategies can be costly and often result in trade-offs with other host fitness parameters such as growth, reproduction, and survival (Beck et al. 1984; Boots and Bowers 1999; Bowers et al. 1994; Sandland and Minchella 2003b). Alternatively, hosts may express strategies that allow parasite infection, but reduce fitness costs associated with invasion through reproductive enhancement (termed "fecundity compensation") (Minchella and Loverde 1981; Sandland and Minchella 2004) or suppression of resistance responses which themselves can cause host damage and pathogenicity (termed "tolerance"). Recently, a study by Miller et al. (2005) investigated the evolutionary consequences of hosts employing two different strategies in the face of infection: control, in which hosts reduced infection pathogenicity by actively reducing parasite replication rates, and tolerance, where hosts accommodated infection but did not reduce pathogen replication rates. Differences in the strategies exhibited by different species or strains of host, can significantly influence parasite evolution (Zhang et al. 2007b). Although this scenario is of great interest from an evolutionary standpoint, it is challenging mathematically.

The study presented in this paper investigates the evolutionary outcomes of interactions between a complex life-cycle parasite (*S. mansoni*) and its hosts (humans and snails). Schistosomes are dioecious helminth parasites with indirect life cycles. Although several species of parasite compose the genus *Schistosoma*, we focus on *Schistosoma mansoni*, a parasite of great human concern as it causes morbidity and mortality in over 200 million people worldwide (CDC—Schistosomiasis Fact Sheet 2011; Chitsulo et al. 2000). *S. mansoni* uses snails along with humans to complete its life cycle. Adult (female) worms within human hosts produce eggs, which, hatch into miracidia when they come in contact with water. These larvae (miracidia) can

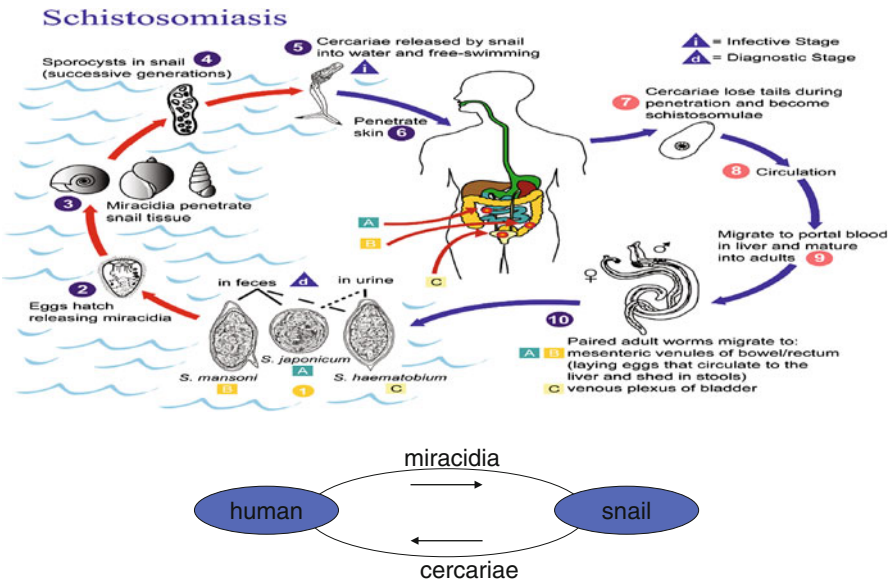

Fig. 1 A diagram showing the schistosome life cycle (CDC—Schistosomiasis Biology 2011). The parasite uses both the human (definitive) host and the snail (intermediate) host to complete its development

then infect snails. After 5 weeks, parasites (cercariae) are released from snails and are infective to human hosts (see Fig. 1).

Schistosome infections of humans are often controlled through chemotherapy using praziquantel (PZQ), a chemical that reduces human morbidity by killing adult worms and diminishing the egg deposition within treated human hosts. Current evidence supports the view that selection for resistance to PZQ may be occurring in schistosome populations and natural schistosome strains exhibit varying resistance to treatment with PZQ (Cioli 2000; Fallon et al. 1997; Ismail et al. 1999). Due to the age-dependence in schistosome infections in humans, various age-targeted treatment strategies have been adopted in different populations, and mathematical models have been used to assess the cost-effectiveness of the disease control programs (Chan et al. 1995; Zhang et al. 2007a).

Our model considered in this paper includes explicitly both the definitive human host and the intermediate snail host. An age-structure is used for the human population to take into account the age-dependent rates of infection and drug treatment. To study the evolution of resistance to infection in the snail population, we consider two types of snail hosts, one being more susceptible (sensitive to infection) and the other one being more resistant to parasite infection. The parasite populations at the free-living stages are modeled implicitly through the adult parasites and infected snails. The model consists of a system of differential and integral equations. By conducting stability analyses of the system we obtain threshold conditions, which are then used to derive criteria for invasion by different host types. To study the evolution of parasite-resistance in the snail host, we adopt the approach of using pairwise-invasibility plots (PIP) (Geritz et al. 1997, 1998; Metz et al. 1996) to explore the evolutionary stable

strategy (ESS). Several trade-off relationships between model parameters are considered based on biological evidence. Our model results help provide valuable insights into this biological system. For example, the results can be used to determine how the evolutionary outcomes of the system may depend on biological factors including the shapes of the trade-off functions, the age-dependent rates of infection and drug treatment in the human host, the level of drug-resistance of the parasite, and the prevalence of infection (see Sect. 4).

2 The model

Let $n(t,a)$ denote the density function of human hosts of age a at time t, and let $p(t,a)$ denote the density function of parasites carried by human hosts of age a at time t. Based on the models in Anderson and May (1978), Dobson (1988), Hadeler (1984), Hadeler and Dietz (1983), and Zhang et al. (2007a), the equations for $n(t,a)$ and $p(t,a)$ take the forms (a derivation of these equations is given in the Appendix):

$$\begin{aligned}
&\frac{\partial}{\partial t}n(t,a)+\frac{\partial}{\partial a}n(t,a)=-\mu_h(a)n(t,a),\\
&\frac{\partial}{\partial t}p(t,a)+\frac{\partial}{\partial a}p(t,a)=\beta(a)n(t,a)C(t)-\big(\mu_h(a)+\mu_p+f(\sigma(a))\big)\,p(t,a),\\
&n(t,0)=\Lambda_h,\ n(0,a)=n_0(a),\ p(t,0)=0,\ p(0,a)=p_0(a).
\end{aligned}\tag{1}$$

The parameters $\mu_h(a)$ and μ_p denote the per capita natural death rates of human hosts of age a and the adult parasites within human hosts, respectively; $f(\sigma(a))$ is the age-dependent killing rate of parasites due to effective drug treatment strategy $\sigma(a)$ for humans; $\beta(a)$ is the per capita infection rate of human hosts by cercariae. $C(t)$ is the density of free-swimming cercariae released by infected snail hosts, whose form will be specified later. The boundary conditions are $n(t,0)=\Lambda_h$ (birth rate of human hosts) and $p(t,0)=0$ (humans are born uninfected), and initial conditions are $n(0,a)=n_0(a)$ and $p(0,a)=p_0(a)$ for given bounded functions with compact supports. Note that in the $n(t,a)$ equation in (1) the parasite-induced death rate has been ignored. This is because the disease mortality in humans is low and the main focus of this study is on the evolution of parasite-resistance in the snail host.

For the snail population, we consider two types of snail hosts based on their susceptibility to infection by the parasite with type 1 being more susceptible and type 2 being more resistant. Each type of the snail populations is divided into two sub-classes: uninfected ($S_k, k=1,2$) and infected ($I_k, k=1,2$). Following the model structure in Zhang et al. (2007a) (the model there includes only a single type of snail host), the disease dynamics of the snail population is described by the following ordinary differential equations:

$$\begin{aligned}
\frac{d}{dt}S_k(t)&=\frac{b_{1k}S_k(t)}{b_{2k}+\sum_{i=1,2}[S_i(t)+I_i(t)]}-\rho_k M(t)S_k(t)-\mu_s S_k(t),\\
\frac{d}{dt}I_k(t)&=\rho_k M(t)S_k(t)-(\mu_s+\delta_k)I_k(t),\quad k=1,2.
\end{aligned}\tag{2}$$

The density-dependent growth rate

$$\frac{b_{1k}S_k(t)}{b_{2k}+\sum_{i=1,2}[S_i(t)+I_i(t)]} \tag{3}$$

corresponds to the competition between the snails for limited resources. More detailed explanations of this form of density dependence can be found in Rueffler and Schreiber (2005). In a comprehensive review of snail–trematode interactions, Sorensen and Minchella (2001) concluded that trematode infection reduces or completely inhibits snail reproductive activity (see also Meuleman 1972; Pan 1965; Sandland and Minchella 2003b). In the case of the interaction between *S. mansoni* and *B. glabrata*, host sterilization has been well documented (see Gerard and Theron 1997) and continues throughout the life time of the snail (see Gerard and Theron 1997; Sorensen and Minchella 2001). Based on these studies, we also assumed in (3) that only uninfected susceptible snails reproduce.

The parameters b_{1k} and $b_{2k}(k = 1, 2)$ are the saturation and scaling constants, respectively, for the type k host. For simplicity the two scaling constants b_{21} and b_{22} are set to be the same. In (2), ρ_k is the per capita infection rate of type k uninfected snail host; μ_s and δ_k are the per capita natural death rate of the snail hosts and the per capita disease-induced death rate of infected snail hosts of type $k(k = 1, 2)$ respectively; and $M(t)$ is the density of the free-living miracidia produced by the adult parasites within the human hosts.

Since miracidia and cercariae die quickly if they cannot find a host to infect (Feng et al. 2004), we assume that $M(t)$ is proportional to the number of adult parasites, i.e.,

$$M(t) = \gamma \int_0^\infty p(t, a)da$$

with γ being the per capita effective egg-production rate of adult female parasites, and that $C(t)$ is proportional to the infected snail hosts, i.e.,

$$C(t) = \sum_{k=1,2} c_k I_k(t)$$

with c_k being the rate at which a type k infected snail host releases cercariae.

Combining the systems (1) and (2) we arrive at the following model:

$$\begin{aligned}
&\frac{\partial}{\partial t}n(t, a) + \frac{\partial}{\partial a}n(t, a) = -\mu_h(a)n(t, a),\\
&\frac{\partial}{\partial t}p(t, a) + \frac{\partial}{\partial a}p(t, a) = \beta(a)n(t, a)C(t) - \left(\mu_h(a) + \mu_p + f(\sigma(a))\right)p(t, a),\\
&\frac{d}{dt}S_k(t) = \frac{b_{1k}S_k(t)}{b_{2k}+\sum_{i=1,2}[S_i(t)+I_i(t)]} - \rho_k M(t)S_k(t) - \mu_s S_k(t),\\
&\frac{d}{dt}I_k(t) = \rho_k M(t)S_k(t) - (\mu_s + \delta_k)I_k(t), \quad k = 1, 2,
\end{aligned} \tag{4}$$

Table 1 Definition of parameters used in the model (4)

Symbol	Definition
$\mu_h(a)$	Per capita natural death rate of human hosts of age a
$\sigma(a)$	Effective drug-treatment rate of human hosts of age a
θ	Drug-resistance level of adult parasite within human hosts
Λ_h	Birth rate of human hosts
$\beta(a)$	Per capita infection rate of human hosts by free-living cercariae
γ	Per capita effective egg-production rate of adult parasites
b_{1k}	Saturation constant for the growth rate of snails
b_{2k}	Scaling constant for the growth rate of snails
ρ_k	Per capita infection rate of type k susceptible snail hosts
c_k	Cercaria releasing rate of an infected snail hosts of type k
μ_s	Per capita natural death rate of snail hosts
μ_p	Per capita natural death rate of adult parasites
δ_k	Per capita disease-induced death rate of infected snail hosts of type k

$k = 1, 2$

$$C(t) = \sum_{k=1,2} c_k I_k(t), \quad M(t) = \gamma \int_0^\infty p(t,a)da,$$
$$n(t,0) = \Lambda_h, \ n(0,a) = n_0(a), \ p(t,0) = 0, \ p(0,a) = p_0(a).$$

All parameters used in the model (4) are listed in Table 1.

3 Mathematical properties of the system (4)

In this section, we study the dynamical behaviors of the system (4) by analyzing the mathematical properties of the system, including the existence and stability of biologically feasible equilibrium points and possible bifurcations. Using a similar approach as in Zhang et al. (2007a) we can show that solutions of the system (4) are defined for all $t \geq 0$ and will remain nonnegative and bounded for all time.

Since the $n(t,a)$ equation in the system (4) is independent of other variables, we can solve it by integrating the equation along the characteristic lines:

$$n(t,a) = \begin{cases} \Lambda_h \pi_h(a), & t \geq a, \\ n_0(a-t)\frac{\pi_h(a)}{\pi_h(a-t)}, & t < a, \end{cases} \tag{5}$$

where $n_0(a)$ is a given function and

$$\pi_h(a) = e^{-\int_0^a \mu_h(w)dw} \tag{6}$$

represents the survival probability of a definitive host of age a. Substituting the solution (5) for $n(t,a)$ in the $p(t,a)$ equation in (4), and integrating the equation we get

$$p(t,a) = \begin{cases} p_1(t,a), & t \geq a, \\ p_2(t,a), & t < a \end{cases} \tag{7}$$

with

$$p_1(t,a) = \Lambda_h \int_0^a \beta(w) C(t+w-a)\pi_h(w) \frac{\pi_\sigma(a)}{\pi_\sigma(w)} dw,$$

$$p_2(t,a) = p_0(a-t)\frac{\pi_\sigma(a)}{\pi_\sigma(a-t)} + \int_{a-t}^a \beta(w) C(t+w-a) n_0(a-t) \frac{\pi_\sigma(a)}{\pi_\sigma(w)} \frac{\pi_h(w)}{\pi_h(a-t)} dw,$$

where

$$\pi_\sigma(a) = e^{-\int_0^a [\mu_h(w)+\mu_p+f(\sigma(w))]dw} \tag{8}$$

represents the survival probability of an adult parasite in a definitive host of age a.

Our approach is to replace the partial differential equations in (4) by integral equations and then analyze the limiting system as $t \to \infty$ of the resulting equations. For this purpose, we rewrite the function $M(t)$ as

$$M(t) = \gamma \int_0^\infty p(t,a)da = \gamma \int_0^t p_1(t,a)da + \gamma \int_t^\infty p_2(t,a)da.$$

Notice that the solutions of the system (4) are bounded. Thus, the last integral in the above expression goes to zero as $t \to \infty$. Let $\tilde{M}(t)$ be the limiting function of $M(t)$, i.e.,

$$\tilde{M}(t) = \gamma \int_0^\infty p_1(t,a)da.$$

Then, by changing the orders of integrations we obtain

$$\begin{aligned} \tilde{M}(t) &= \gamma \int_0^\infty p_1(t,a)da \\ &= \gamma \int_0^\infty \Lambda_h \int_0^a \beta(w) C(t+w-a)\pi_h(w)\pi_\sigma(a)\pi_\sigma^{-1}(w) dw da \end{aligned}$$

$$
\begin{aligned}
&= \gamma \Lambda_h \int_0^\infty \int_w^\infty \beta(w) C(t+w-a) \pi_h(w) \pi_\sigma(a) \pi_\sigma^{-1}(w) da dw \\
&= \gamma \Lambda_h \int_0^\infty \int_0^\infty \beta(w) C(t-\tau) \pi_h(w) \pi_\sigma(w+\tau) \pi_\sigma^{-1}(w) d\tau dw \\
&= \gamma \Lambda_h \int_0^\infty C(t-\tau) \int_0^\infty \beta(w) \pi_h(w) \pi_\sigma(w+\tau) \pi_\sigma^{-1}(w) dw d\tau \\
&= \sum_{k=1,2} c_k \int_0^\infty I_k(t-\tau) R_h(\tau) d\tau,
\end{aligned}
$$

where

$$
R_h(\tau) = \gamma \Lambda_h \int_0^\infty \beta(w) \pi_h(w) \pi_\sigma(w+\tau) \pi_\sigma^{-1}(w) dw. \tag{9}
$$

Substituting $\tilde{M}(t)$ for $M(t)$ in the S_k and I_k equations in system (4), we get the following limiting system for S_k and I_k, which are independent of the variables $n(t,a)$ and $p(t,a)$:

$$
\begin{aligned}
\frac{d}{dt} S_k(t) &= \frac{b_{1k} S_k(t)}{b_{2k} + \sum_{i=1,2} (S_i(t) + I_i(t))} - \rho_k \tilde{M}(t) S_k(t) - \mu_s S_k(t), \\
\frac{d}{dt} I_k(t) &= \rho_k \tilde{M}(t) S_k(t) - (\mu_s + \delta_k) I_k(t), \quad k = 1, 2, \\
\tilde{M}(t) &= \sum_{k=1,2} c_k \int_0^\infty I_k(t-a) R_h(a) da.
\end{aligned} \tag{10}
$$

From (5), (7), and $C(t) = \sum_{k=1,2} c_k I_k(t)$ we know that as $t \to \infty$,

$$
\begin{aligned}
&n(t,a) \to \Lambda_h \pi_h(a), \\
&p(t,a) \to \Lambda_h \int_0^a \beta(w) \left[\sum_{k=1,2} c_k I_k(t+w-a) \right] \pi_h(w) \frac{\pi_\sigma(a)}{\pi_\sigma(w)} dw,
\end{aligned}
$$

where $\pi_h(a)$ and $\pi_\sigma(a)$ are given in (6) and (8). Thus, the asymptotic behaviors of $n(t,a)$ and $p(t,a)$ can be determined once the behaviors of $I_k(t)$ $(k = 1, 2)$ are known. Since the qualitative behaviors of the system (4) can be captured by its limiting system as $t \to \infty$, we will focus in the following subsections on the analysis of the limiting system (10).

3.1 The reduced system with a single type of snail host

System (10) consists of four nonlinear integral-differential equations. It is rather challenging to analyze the qualitative behaviors directly, especially for the existence and stability of a coexistence equilibrium (where all variables are positive). We adopt the approach of considering first the qualitative behaviors of the boundary equilibrium points of the system (10), at which only one type of snail hosts exists (both uninfected and infected snails are present). We then use these results to gain information about a coexistence equilibrium, as well as questions related to invasion and evolution.

In the case when only one type (type 1 or 2) snail host is present, the system (10) reduces to

$$\begin{aligned}
\frac{d}{dt}S_k(t) &= \frac{b_{1k}S_k(t)}{b_{2k}+S_k(t)+I_k(t)} - \rho_k\tilde{M}_k(t)S_k(t) - \mu_s S_k(t),\\
\frac{d}{dt}I_k(t) &= \rho_k\tilde{M}_k(t)S_k(t) - (\mu_s+\delta_k)I_k(t),\\
\tilde{M}_k(t) &= c_k\int_0^\infty I_k(t-a)R_h(a)da, \quad k=1 \text{ or } 2.
\end{aligned} \tag{11}$$

Notice that the only difference between the systems (10) and (11) is between $\tilde{M}(t)$ (which is a sum of two terms) and $\tilde{M}_k(t)$ (which has a single term). Due to the mathematical symmetry between the two types of snail hosts, the analysis of system (11) for $k=1$ and for $k=2$ will be identical. Consider the order of variables of the system (11) to be (S_k, I_k). Since the carrying capacity of the type k snail host in the absence of infection is $\frac{b_{1k}}{\mu_s} - b_{2k}$, we need to assume that

$$\frac{b_{1k}}{\mu_s} - b_{2k} > 0, \quad k=1,2 \tag{12}$$

so that the snail population size is positive in the absence of infection. The system (11) always has the parasite-free equilibrium $E_{k0} = (S_{k0}, 0) = (b_{1k}/\mu_s - b_{2k}, 0)$.

Let $\bar{E}_k = (\bar{S}_k, \bar{I}_k)$ denote an equilibrium of the system (11). Then $\bar{E}_k$ satisfies the equations

$$\frac{b_{1k}\bar{S}_k}{b_{2k}+\bar{S}_k+\bar{I}_k} - \rho_k c_k \mathcal{R}_h \bar{I}_k\bar{S}_k - \mu_s\bar{S}_k = 0, \tag{13}$$

$$\rho_k c_k \mathcal{R}_h \bar{I}_k\bar{S}_k - (\mu_s+\delta_k)\bar{I}_k = 0, \tag{14}$$

where

$$\mathcal{R}_h = \int_0^\infty R_h(\tau)d\tau$$

and $R_h(\tau)$ is given in (9). We can show that the existence of an interior equilibrium (i.e., all components are positive) depends on the parasite reproduction number $\Re_k$ within the type k snail host, which is defined as

$$\Re_k = \frac{\rho_k c_k \mathcal{R}_h}{\mu_s + \delta_k} \left(\frac{b_{1k}}{\mu_s} - b_{2k} \right). \tag{15}$$

Notice from the expression of $R_h(\tau)$ (see (9)) that

$$\beta(w)\Lambda_h \pi_h(w)$$

represents the average number of adult parasites within human hosts of age w produced by one cercariae, and

$$\pi_\sigma(w+\tau)\pi_\sigma^{-1}(w)$$

is the survival probability of an adult parasite in a human host of age $w+\tau$ who was infected τ time units ago while at age w (i.e., τ is the infection age of a human host of age $w+\tau$). Thus, the quantity

$$\int_0^\infty \beta(w)\Lambda_h \pi_h(w)\pi_\sigma(w+\tau)\pi_\sigma^{-1}(w)dw$$

gives the total number of adult parasites within human hosts with infection age τ produced by one cercariae, and $\mathcal{R}_h(\tau)$ gives the total number of miracidia produced by adult parasites within human hosts due to one cercariae. Finally, from the definitions of ρ_k (per capita infection rate of snails of type k), c_k (cercaria releasing rate by one infected snail of type k), $\mu_s + \delta_k$ ($1/(\mu_s + \delta_k)$ is the duration of infection of a snail of type k), and $b_{1k}/\mu_s - b_{2k}$ (size of snails of type k in a susceptible population), we know that $\Re_k$ represents the total number of secondary cercaria produced by one cercariae. That is, $\Re_k$ indeed is the parasite's reproduction number associated with the type k snail hosts.

Let $E_k^* = (S_k^*, I_k^*)$ denote an interior equilibrium of the system (11). From (13) and (14), we have

$$S_k^* = \frac{\mu_s + \delta_k}{\rho_k c_k \mathcal{R}_h} = \frac{1}{\Re_k} \left(\frac{b_{1k}}{\mu_s} - b_{2k} \right), \tag{16}$$

and I_k^* satisfies the equation

$$\frac{b_{1k}}{b_{2k} + S_k^* + I_k^*} - \rho_k c_k \mathcal{R}_h I_k^* - \mu_s = 0. \tag{17}$$

Equation (17) can be rewritten as

$$F(I_k^*) = 0, \tag{18}$$

where $F(x)$ is a quadratic function defined by

$$F(x) = \rho_k c_k \mathcal{R}_h x^2 + \left[\rho_k c_k \mathcal{R}_h (b_{2k} + S_k^*) + \mu_s\right] x + \mu_s (b_{2k} + S_k^*) - b_{1k},$$

and S_k^* is given in (16). Notice that

$$\begin{aligned} F(0) &= \mu_s (b_{2k} + S_k^*) - b_{1k} \\ &= \mu_s \left(b_{2k} + \frac{\mu_s + \delta_k}{\rho_k c_k \mathcal{R}_h} \right) - b_{1k} \\ &= \frac{\mu_s (\mu_s + \delta_k)}{\rho_k c_k \mathcal{R}_h} \left[1 - \frac{\rho_k c_k \mathcal{R}_h}{\mu_s + \delta_k} \left(\frac{b_{1k}}{\mu_s} - b_{2k} \right) \right] \\ &= \frac{\mu_s (\mu_s + \delta_k)}{\rho_k c_k \mathcal{R}_h} (1 - \Re_k). \end{aligned}$$

Clearly, $F(0) < 0$ (> 0) when $\Re_k > 1$ (< 1). Notice also that $F(x)$ has a minimum at

$$x_{\min} = -\frac{\rho_k c_k \mathcal{R}_h (b_{2k} + S_k^*) + \mu_s}{2\rho_k c_k \mathcal{R}_h} < 0.$$

This implies that the equation $F(x) = 0$ has a unique positive solution for $\Re_k > 1$ and no positive solution for $\Re_k < 1$. Thus, we have the following result:

Result 1 *There is a unique interior equilibrium E_k^* when $\Re_k > 1$, and E_k^* does not exist when $\Re_k < 1$.*

The next result shows that the reproduction number $\Re_k$ and the threshold value $\Re_k = 1$ also determine the stabilities of the equilibrium points E_{k0} and E_k^* of the system (11).

Result 2 *Assume that the condition (12) holds.*

(a) *The parasite-free equilibrium $E_{k0} = \left(\frac{b_{1k}}{\mu_s} - b_{2k}, 0\right)$ is locally asymptotically stable if $\Re_k < 1$, and it is unstable if $\Re_k > 1$.*

(b) *When $\Re_k > 1$, there exists a threshold value $b_{1k} = \tilde{b}_{1k}$ (with all other parameters being fixed), such that the unique endemic equilibrium $E_k^* = (S_k^*, I_k^*)$ determined in Result 1 is locally asymptotically stable if $b_{1k} < \tilde{b}_{1k}$.*

Moreover, numerical simulations show that a Hopf bifurcation may occur at some critical point $b_{1k} = b_{1k}^* > \tilde{b}_{1k}$, leading to the appearance of stable periodic solutions.

The analytic proofs for Part (a) and Part (b) of Result 2 are provided in the Appendix. The existence of a Hopf bifurcation and the threshold point b_{1k}^* is confirmed via numerical simulations. This is illustrated in Fig. 2, which shows numerical solutions of the fraction $\frac{I_k(t)}{S_k(t)+I_k(t)}$ for two values of b_{1k} below or above b_{1k}^* ($k = 1$ or 2). The solution converges to the equilibrium E_k^* when $b_{1k} < b_{1k}^*$ (see (a)), and a stable periodic solution exists for $b_{1k} > b_{1k}^*$ (see (b)). Other parameter values used in the simulations are: $\Lambda_h = 8$, $\mu_h = 0.014$, $\mu_s = 0.5$, $\delta_k = 1.8$, $\mu_p = 0.2$, $\beta_0 = 2 \times 10^{-5}$, $\rho_k = 10^{-4}$, $\gamma_0 = 3$, $b_{2k} = 600$ and $c_k = 20{,}000$ ($k = 1, 2$). The time unit is year. Most of the values are from Feng et al. (2004), and the definitions of β_0 and γ_0 are given in Sect. 4.1.

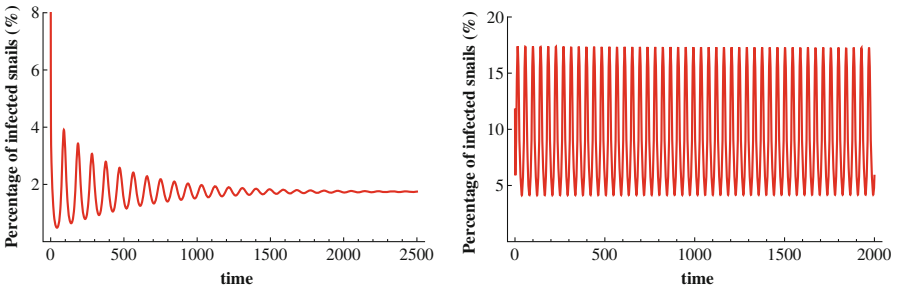

(a) Simulation result for $b_{1k} < b_{1k}^*$. **(b)** Simulation result for $b_{1k} > b_{1k}^*$.

Fig. 2 Time plots of the fraction of infected snail hosts $\frac{I_k(t)}{S_k(t)+I_k(t)}$ for the reduced system (11) with a single type of snail host ($k = 1$ or 2). The plot in **a** is for the case when the parameter values are chosen such that $\Re_k > 1$ and $b_{1k} = 330 < b_{1k}^*$. It shows that the equilibrium E_k^* is stable. The plot in **b** is for the case when $\Re_k > 1$ and $b_{1k} = 450 > b_{1k}^*$. It shows that a stable periodic orbit exists. Other parameter values are given in the *text*

3.2 Analysis of the model with both types of snail hosts

In this section, we study the dynamics of the full system (10) in which both types of snail hosts are included. As we have mentioned earlier, an interior equilibrium of the reduced system (11) corresponds to a boundary equilibrium of the full system (10). Again, we omit the extreme case when both snail populations are absent. Using the order of variables $U = (S_1, I_1, S_2, I_2)$ and from the results in Sect. 3.1, we know that the system (10) has the following non-trivial boundary equilibrium points:

$$U_{10} = \left(\frac{b_{11}}{\mu_s} - b_{21}, 0, 0, 0\right), \quad U_{02} = (0, 0, \frac{b_{12}}{\mu_s} - b_{22}, 0),$$
$$U_1^* = (S_1^*, I_1^*, 0, 0), \qquad U_2^* = (0, 0, S_2^*, I_2^*),$$

where S_k^* and I_k^* are determined in Sect. 3.1 (see (16)–(18)). The subscript "10" in U_{10} represents the equilibrium at which only type 1 snail host is present and there is no infection. Similarly, the subscript "02" in U_{02} represents the equilibrium with type 2 snail host only and without infection. The system (10) may also have other boundary equilibria. However, for the biological questions we are interested in, we will only consider the ones listed above.

An interior equilibrium of system (10), denoted by $U^\diamond = (S_1^\diamond, I_1^\diamond, S_2^\diamond, I_2^\diamond)$ with all components positive, satisfies the following system of four equations

$$\frac{b_{1k} S_k{}^\diamond}{b_{2k} + \sum_{i=1,2}(S_i{}^\diamond + I_i{}^\diamond)} - \rho_k M^\diamond S_k^\diamond - \mu_s S_k{}^\diamond = 0,$$
$$\rho_k M^\diamond S_k{}^\diamond - (\mu_s + \delta_k) I_k{}^\diamond = 0, \quad k = 1, 2,$$

where $M^\diamond = \sum_{i=1,2} c_i I_i{}^\diamond \mathcal{R}_h$. It is very difficult to solve analytically the above system for $U^\diamond$. This is the main reason that we will study questions related to the coexistence equilibria via numerical simulations.

It turns out that a degenerate case occurs (i.e., the characteristic equation at the parasite-free equilibrium U_{10} or U_{02} has a zero eigenvalue) when the two types of snail hosts have the same carrying capacity, i.e., when

$$\frac{b_{11}}{\mu_s} - b_{21} = \frac{b_{12}}{\mu_s} - b_{22}.$$

Thus, when discussing the stability of U_{10} or U_{02}, we assume that the two carrying capacities are not equal. Without loss of generality, assume that the type 1 snail host has a higher carrying capacity, i.e.,

$$\frac{b_{11}}{\mu_s} - b_{21} > \frac{b_{12}}{\mu_s} - b_{22} > 0. \tag{19}$$

Under this condition we have the following result.

Result 3 *Let the condition* (19) *hold.*

(a) U_{10} *is locally asymptotically stable when* $\Re_1 < 1$ *and unstable when* $\Re_1 > 1$.
(b) U_{02} *is always unstable.*

A proof of Result 3 can be found in the Appendix.

The more interesting results are about the stabilities of U_1^* and U_2^*, as these results are directly related to the invasion properties of a population. For example, the stability of the equilibrium E_1^* for the reduced system (11) indicates that the snail population of type 1 has stabilized at the equilibrium U_1^* for the full system (10) in the absence of snails of type 2. When a small number of new species of snails (type 2) is introduced into this environment, they will be able to invade into the population of host type 1 only if the equilibrium U_1^* for the full system (10) is unstable. In such a case, we refer to the snail host of type 1 as the "resident host" and the snail host of type 2 as the "mutant host", and refer to this invasion as invasion of U_1^* by the mutant host.

We first derive the invasion condition using the invasibility analysis (see Bowers 1999; Bowers and Turner 1997). A mathematical proof of the result will be provided at the end of this section. In order for the mutant snails to successfully invade U_1^*, they must have a positive growth rate. In the process of invasion by a susceptible mutant snail, the snail may either remain uninfected or become infected if it did not die. Let T_U denote the average duration in which the snail is alive and uninfected. Then

$$T_U = \frac{1}{\mu_s + \rho_2 c_1 I_1^* \mathcal{R}_h}.$$

Let T_I denote the average duration of being infected (and did not die). Note that the lifespan of an uninfected (infected) snail of type 2 is $1/\mu_s$ ($1/(\mu_s + \delta_2)$), and that

$$\frac{T_U}{1/\mu_s} + \frac{T_I}{1/(\mu_s + \delta_2)} = 1. \tag{20}$$

From the Eq. (20) we have

$$T_I = \frac{\rho_2 c_1 I_1^* \mathcal{R}_h}{(\mu_s + \delta_2)(\mu_s + \rho_2 c_1 I_1^* \mathcal{R}_h)}.$$

Let ϕ_U and ϕ_I denote the net contribution of the snail to the growth rate of the population during the periods T_U and T_I respectively. Recall the assumption that infected snails do not reproduce. Thus,

$$\begin{aligned} \phi_U &= \frac{b_{12}}{b_{22} + S_1^* + I_1^*} - \mu_s, \\ \phi_I &= -(\mu_s + \delta_2). \end{aligned}$$

Then, the total contribution of the snail to the population growth of the mutant type is

$$\begin{aligned} g_2 &= \phi_U T_U + \phi_I T_I \\ &= \left(\frac{b_{12}}{b_{22} + S_1^* + I_1^*} - \mu_s \right) \frac{1}{\mu_s + \rho_2 c_1 I_1^* \mathcal{R}_h} - \frac{(\mu_s + \delta_2)\rho_2 c_1 I_1^* \mathcal{R}_h}{(\mu_s + \delta_2)(\mu_s + \rho_2 c_1 I_1^* \mathcal{R}_h)} \\ &= \frac{\frac{b_{12}}{b_{22} + S_1^* + I_1^*}}{\mu_s + \rho_2 c_1 I_1^* \mathcal{R}_h} - 1. \end{aligned} \tag{21}$$

Clearly, g_2 must be positive in order for the mutant type to successfully invade the resident population. From the condition $g_2 > 0$ we obtain the invasion reproduction number $\Re_{21}$ and the invasion condition:

$$\Re_{21} = \frac{\frac{b_{12}}{b_{22} + S_1^* + I_1^*}}{\mu_s + \rho_2 c_1 I_1^* \mathcal{R}_h} > 1. \tag{22}$$

The interpretation of $\Re_{21}$ is clear. The fraction $\frac{b_{12}}{b_{22} + S_1^* + I_1^*}$ gives the number of new mutant snails produced by one susceptible snail of type 2 while the type 1 snail host is at the equilibrium U_1^*, and $\frac{1}{\mu_s + \rho_2 c_1 I_1^* \mathcal{R}_h} = T_U$ is the duration in which the mutant snail is productive (i.e., alive and uninfected). Thus, $\Re_{21}$ represents the net reproduction number of the mutant host in the environment where the resident host is at the equilibrium U_1^*.

By symmetry, we can also obtain the condition under which the type 1 host (as the mutant) can invade U_2^* is

$$\Re_{12} = \frac{\frac{b_{11}}{b_{21} + S_2^* + I_2^*}}{\mu_s + \rho_1 c_2 I_2^* \mathcal{R}_h} > 1, \tag{23}$$

here $\Re_{12}$ is the invasion reproduction number for the type 1 snail host.

Remark We point out that the quantity $\Re_k$ (for $k = 1, 2$) is a measure of the parasite's reproduction associated with the type k snail host, whereas the quantity $\Re_{ji}$

$(1 \leq i \neq j \leq 2)$ is a measure of the snail host's reproduction. More precisely, $\Re_{ji}$ describes the reproductive ability of type j snails when introduced to an environment where the type i host is at the endemic equilibrium with $S_i^* > 0$ and $I_i^* > 0$. We also need to point out that the Eq. (22) also provides an equivalent version of fitness for the mutant host. As discussed in Hoyle and Bowers (2008), the fitness is defined as being the per capita growth rate of a rare mutant invader (see Metz et al. 1992). A sign-equivalent version of it is given by $\Re_0 - 1 > 0$, where $\Re_0$ is the dominant eigenvalue of the next generation matrix as defined in Diekmann and Heesterbeek (2000). The quantity $\Re_{21}$ given in (22) has a similar meaning.

Using these invasion reproduction numbers we can describe the stability results for U_k^* $(k = 1, 2)$ as follows.

Result 4 *Let* $b_{11} < \tilde{b}_{11}$ (*this will exclude the possibility of periodic orbits in the reduced system* (3.1)*, see Result* 2).

(a) *The equilibrium* U_1^* *exists if the basic reproduction number* $\Re_1 > 1$.
(b) U_1^* *is locally asymptotically stable if the invasion reproduction number* $\Re_{21} < 1$ *and unstable if* $\Re_{21} > 1$.

A symmetric result also holds:

Result 5 *Let* $b_{12} < \tilde{b}_{12}$.

(a) *The equilibrium* U_2^* *exists if the basic reproduction number* $\Re_2 > 1$.
(b) U_2^* *is locally asymptotically stable if the invasion reproduction number* $\Re_{12} < 1$ *and unstable if* $\Re_{12} > 1$.

A proof of Result 4 can be found in the Appendix. Result 5 can be proved in a similar way.

We remark that Results 4 and 5 imply that the coexistence of both types of snail hosts with a positive infection level will be expected when both invasion reproduction numbers exceed 1, i.e., $\Re_{21} > 1$ and $\Re_{12} > 1$. This is illustrated in Fig. 3a. However, these are only sufficient but not necessary conditions. This is because in Results 4 and 5, there are other conditions such as $\Re_1 > 1$ or $\Re_2 > 1$ (they ensure the existence of U_1^* or U_2^*). Thus, coexistence may still be possible even when one of the invasion reproduction numbers is below 1, e.g., $\Re_{12} < 1$ and $\Re_{21} > 1$. One of such cases is illustrated in Fig. 3b. In the case when U_1^* and U_2^* both exist and are stable, coexistence cannot occur if one of the invasion reproduction numbers is below 1. This is illustrated in Fig. 4.

We remark also that although the outcome of competitive-exclusion between the two types of snail hosts is expected without the shared parasite, it may not be the case in the presence of parasites. This is why the condition $\Re_k > 1$ is required, which guarantees the establishment of the parasite population in the type k snail host. Notice that the conditions for coexistence depend on the invasion reproduction numbers $\Re_{12}$ and $\Re_{21}$ which, from (22) and (23), depend on the levels of infection in the two types of snail hosts.

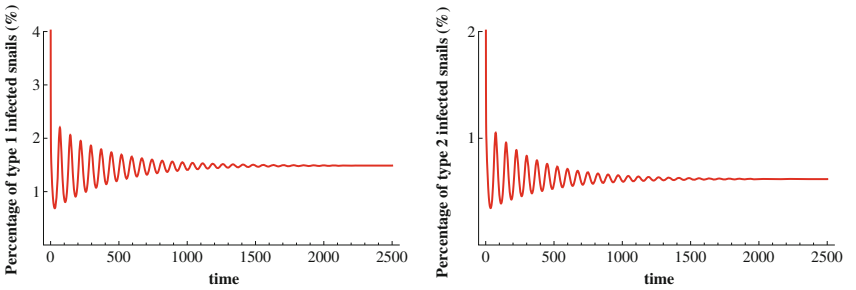

(a) Time plots for the case when $\Re_{12} > 1$ and $\Re_{21} > 1$, i.e., both invasion reproduction numbers exceed 1.

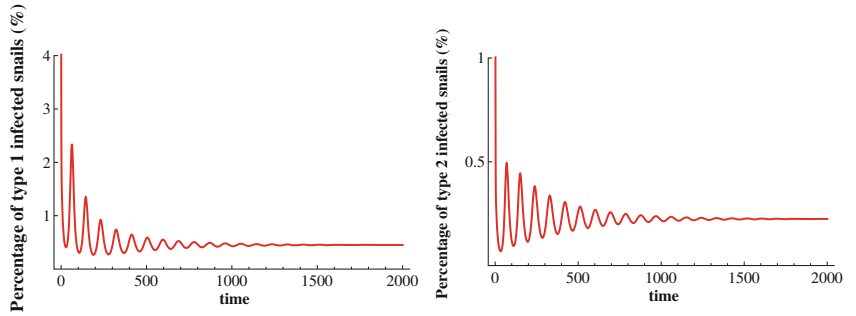

(b) Time plots for the case when $\Re_{12} < 1$ and $\Re_{21} > 1$, i.e., one invasion reproduction number is below 1.

Fig. 3 Time plots of the fractions of infected snail hosts $\frac{I_k(t)}{\sum_{i=1,2}(S_i(t)+I_i(t))}$ of type k ($k = 1, 2$) for the full system (4). Plots in **a** are for the case when both $\Re_{12}$ and $\Re_{21}$ are greater than 1, whereas plots in **b** are for the case when $\Re_{12} < 1$ and $\Re_{21} > 1$. In both cases, the system converges to the endemic equilibrium $U^{\diamond}$. All parameter values are the same as in Fig. 2 except for ρ_2: $\rho_2 = 3 \times 10^{-5}$ in (a) and $\rho_2 = 10^{-5}$ in (b)

4 Biological insights gained from the model analysis

In this section, we use the mathematical results obtained in previous sections to explore the population outcomes of the two types of snail hosts under the influence of the pathogen. Assuming that there are costs for the snail hosts to be resistant to parasite infection, we can use the invasion thresholds to examine how the differences in host resistance and reproduction may influence the snail population composition. The invasion conditions also allow us to look at the evolutionary trajectories of both hosts and parasites in terms of either parasite-resistance (hosts) or virulence (parasites).

4.1 Competitive outcomes between two types of hosts

We are interested in exploring how the variability in parasite-resistance (and its associated fitness costs) may affect the composition of snail types within a population (e.g., monomorphism vs. coexistence). Outcomes may also depend on the intensity of drug-treatment in human hosts, age-dependent infection rates, and the level of drug-resistance of the parasites.

Consider the type 1 snail host as the resident type which is more susceptible to parasite infection (e.g., with a higher ρ_1 value), and consider the type 2 snail host to

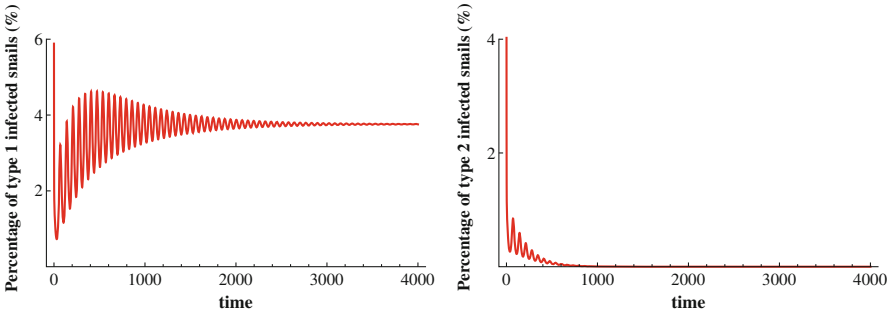

(a) Time plots for the case when $\Re_{12} > 1$ and $\Re_{21} < 1$.

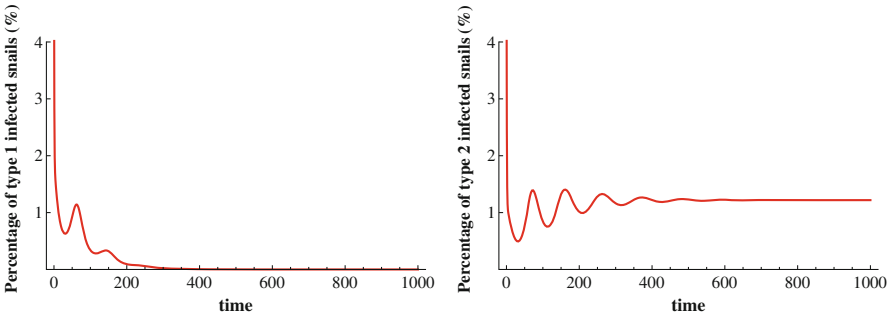

(b) Time plots for the case when $\Re_{12} < 1$ and $\Re_{21} > 1$.

Fig. 4 Similar to Fig. 3b but for the case when both U_1^* and U_2^* are existent and stable ($\Re_1$ and $\Re_2$ are both greater than 1). Plots in **a** show that the system converges to the boundary equilibria U_1^* when $\Re_{12} = 1.13 > 1$ ($b_{12} = 317$) and $\Re_{21} = 0.985 < 1$, whereas plots in **b** show that the system converges to the boundary equilibria U_2^* when $\Re_{12} = 0.95 < 1$ ($b_{12} = 335$) and $\Re_{21} = 1.04 > 1$. All other parameters have the same values as in Fig. 3b

be more resistant to parasite infection (i.e., $\rho_2 < \rho_1$). The trade-off for type 2 hosts is that a higher resistance may result in a reduced birth rate (which is represented by the parameter b_{12}, i.e., $b_{12} < b_{11}$). We will investigate how the changes in ρ_k and b_{1k} ($k = 1, 2$) may affect population outcomes. More specifically, we will examine how the threshold quantities determined by the invasion reproduction numbers, $\Re_{21} = 1$ and $\Re_{12} = 1$, may depend on changes in the two quantities:

$$\frac{\rho_1 - \rho_2}{\rho_1} \quad \text{and} \quad \frac{b_{11} - b_{12}}{b_{11}}. \tag{24}$$

To do this, we need to specify the forms of age-dependent functions in the human hosts such as $\beta(a)$ and $\sigma(a)$, as well as the forms of parasite production as a function of drug-resistance, $\gamma(\theta)$. Here, the age-dependent transmission rate $\beta(a)$ and drug-treatment rate $\sigma(a)$ are chosen as step functions based on epidemiological data which suggest that the highest prevalence of schistosome infection occurs within the age group 11–20 (see Massara et al. 2004; Sturrock 2001). Examples of such functions are:

$$\beta(a) = \begin{cases} \beta_0 \beta_j & \text{if } 10\,(j-1) < a \le 10\,j,\ \ j = 1, 2, \ldots, 7, \\ 0 & \text{if } a > 70 \end{cases} \tag{25}$$

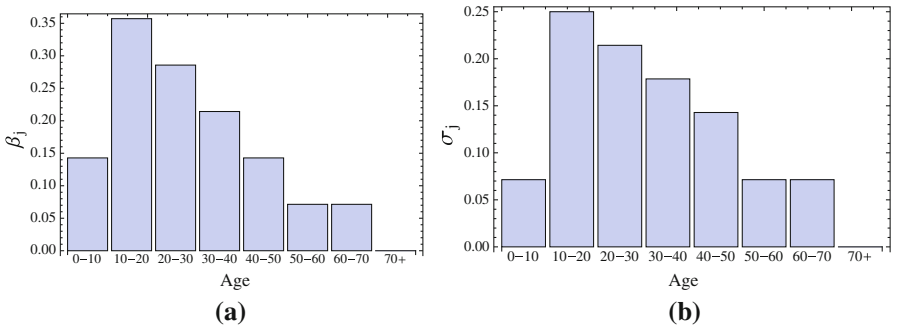

Fig. 5 Examples of β_j and σ_j used in the age-dependent functions $\beta(a)$ and $\sigma(a)$ as defined in (25) and (26). These functions are used in the simulations. **a** Age-dependent transmission $\beta(a)$. **b** Age-dependent drug treatment $\sigma(a)$

and

$$\sigma(a) = \begin{cases} \sigma_0\sigma_j & \text{if } 10(j-1) < a \le 10\,j,\ j = 1, 2, \ldots, 7, \\ 0 & \text{if } a > 70. \end{cases} \tag{26}$$

In these formulas, β_0 and σ_0 represent respectively the background transmission rate and the effective treatment rate of definitive hosts. The constants β_j and σ_j depend on the ages of human hosts (see Zhang et al. 2007a), and examples of these functions are demonstrated in Fig. 5.

The function $f(\sigma(\theta))$ denotes the death rate of parasites due to drug treatment with treatment rate $\sigma(\theta)$ for parasites with a drug-resistant level $\theta \ge 1$ ($\theta = 1$ for drug-sensitive parasites). In our simulations, this death rate is assumed to be

$$f(\sigma(a)) = \frac{\sigma(a)}{\theta}, \quad \theta \ge 1. \tag{27}$$

Based on experimental studies (Gower and Webster 2005), we assume that parasites with drug-resistance level θ have a reduced reproduction rate $\gamma(\theta)$ which reflects the cost of drug-resistance. Two particular forms of $\gamma(\theta)$ considered here are given by

$$\gamma(\theta) = \gamma_0 \left(\frac{9-\theta}{8}\right), \tag{28}$$

$$\gamma(\theta) = \gamma_0 \left(\frac{16-\theta}{15}\right)^{1/5}, \tag{29}$$

where $\gamma_0 > 0$ is a constant representing the background replication rate of drug-sensitive parasites. The curves of these two functions are shown in Fig. 6 for the case of $\gamma_0 = 1$. The solid curve corresponds to the function in (28) which represents the case when the cost for resistance is higher, whereas the dashed curve corresponds to the function in (29) which represents the case when the cost for resistance is lower.

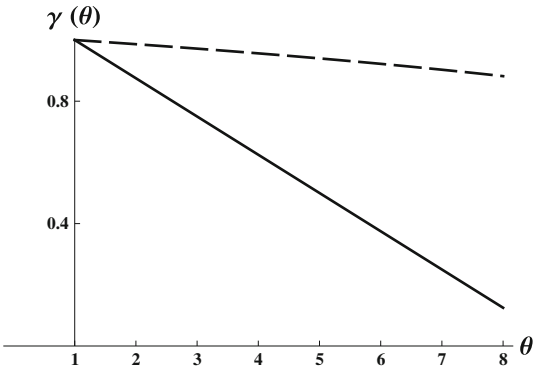

Fig. 6 The effective parasite reproduction rate $\gamma(\theta)$ versus the drug-resistance level θ. The *solid* and *dashed lines* represent the cases of higher and lower costs of drug resistance, respectively

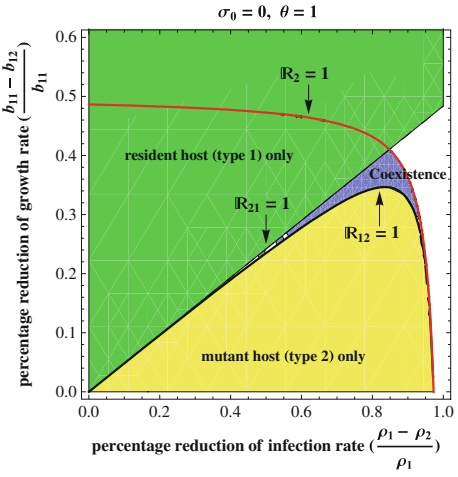

Fig. 7 Competitive outcomes between the parasite-susceptible (resident) strain and the parasite-resistant (mutant) strain of snail hosts in the trade-off space characterized by $\left(\frac{\rho_1-\rho_2}{\rho_1}, \frac{b_{11}-b_{12}}{b_{11}}\right)$. We observe that the mutant type is favored when the cost of parasite-resistance is low, whereas coexistence is favored for intermediate levels of cost. This plot is for the case when there is no drug treatment of humans (i.e., $\sigma_0 = 0$) and drug-resistance is absent (i.e., $\theta = 1$)

Given these functional forms and assumptions specified above, and for fixed values of θ, β_0 and σ_0, we can generate a bifurcation diagram in the parameter plane $\left(\frac{\rho_1-\rho_2}{\rho_1}, \frac{b_{11}-b_{12}}{b_{11}}\right)$ as shown in Fig. 7. In this figure, the infection rate and growth rate for the resident snail host (b_{11} and ρ_1) are fixed, and the corresponding rates for the mutant type snail host (b_{12} and ρ_2) can vary. The fraction $(b_{11} - b_{12})/b_{11}$ provides a measure for the cost of parasite resistance in the snail host, and the fraction $(\rho_1 - \rho_2)/\rho_1$ describes the level of parasite resistance in the snail host. We plotted three curves determined by the equations $\Re_{12} = 1$, $\Re_{21} = 1$ and $\Re_2 = 1$, which divide the plane in three regions. In the region below (above) the $\Re_{12} = 1$ curve, the mutant type host will out-compete (be excluded by) the resident type host. In the region between the three curves (i.e., above the $\Re_{12} = 1$ curve and below the two curves determined by $\Re_{21} = 1$ and $\Re_2 = 1$), coexistence will be expected. Figure 3a is an example of the case when $\Re_{12} > 1$, $\Re_{21} > 1$ and $\Re_2 > 1$, which is in the coexistence region.

We need to point out that the coexistence region described above may not allow for an evolutionary branching point in adaptive dynamics terms, which we will discuss more in Sect. 4.2. Such an example is presented in Bowers et al. (2005). The approach

they presented requires that one can solve the invasion equations (both mutant and resident), which are needed in order to consider their derivatives and the derivatives of trade-offs. A branching point can then be determined by observing in which region the trade-off curve enters the singular TIP (trade-off and invasion plots). For our model, it is not easy to determine the branching point as the invasion equations are difficult to solve analytically. It is possible that the coexistence state in the coexistence region is temporary and unstable, depending on the properties of the evolutionarily singular strategy that are determined by the trade-off assumptions on hosts' benefits and costs (which are shown in the next section).

We also observe in Fig. 7 that for smaller values of $(b_{11} - b_{12})/b_{11}$ (i.e., when cost of resistance is low), mutant snails with a wider rage of resistance (represented by the values of $(\rho_1 - \rho_2)/\rho_1$) can out-compete the resident snails. On the other hand, when cost of resistance is high (larger values of $(b_{11} - b_{12})/b_{11}$), it is more likely that the resident type will exclude the resistance type. Coexistence of both resident and mutant snails is favored only when the cost is at an intermediate level. Other parameter values used in Fig. 7 are: $b_{11} = 600$, $\rho_1 = 10^{-4}$, $\Lambda_h = 8$, $\mu_h = 0.014$, $\mu_s = 0.5$, $\mu_p = 0.2$, $\beta_0 = 10^{-5}$, $\gamma_0 = 3$, $\delta_k = 1.8$, and $c_k = 20{,}000$ $(k = 1, 2)$.

Figure 7 is for the case of no drug treatment for the human host ($\sigma_0 = 0$). When drug treatment is present ($\sigma_0 > 0$), although the qualitative behaviors of the competition between snail types are similar to that presented in Fig. 7, significant quantitative differences can be observed depending on the age-dependent treatment strategies. For example, in Fig. 8, two bifurcation diagrams are plotted for two treatment strategies that target at different age-groups. Figure 8a is for the case when the age-dependent treatment strategy $\sigma(a)$ follows the distribution shown in Fig. 5b, and Fig. 8b is for the treatment strategy that targets only at the age-group 10–30, i.e., $\sigma(a) \neq 0$ only for $10 < a \leq 30$. For the two $\sigma(a)$ functions used in Fig. 8a, b, the areas under the $\sigma(a)$ curve are the same. All other parameters are the same as in Fig. 7. We observe that the targeted treatment strategy (Fig. 8b) makes it more likely for the mutant host type (parasite-resistant) to out-compete the resident type (parasite-susceptible).

We can also view the difference in ρ_k and in b_{1k} $(k = 1, 2)$ as a measure of similarity between the two host types of snails. It shows that if the two snail host types are similar, then monomorphism is favored. As the degree of similarity decreases (bigger differences), the likelihood of polymorphism increases. This seems to suggest that the cost of parasite-resistance may contribute to the maintenance of polymorphism in the presence of the parasite (Bowers et al. 1994; Webster and Woolhouse 1999).

4.2 Evolution of parasite-resistance in snail hosts

In this section, we consider the snail types 1 and 2 as the resident (or susceptible) and mutant (or resistant) hosts, respectively, and replace the subscripts 1 and 2 by s and m to denote resident and mutant. Because this study focuses on the evolution of (snail) host resistance to parasite infection, and the parameter ρ_m represents the infection rate of mutant (resistant) snail host, we thus choose ρ_m for the analysis of evolutionary outcomes. Based on the experimental results in Webster and Woolhouse (1999), we assume that there are some costs associated with the host's resistance to parasites. For

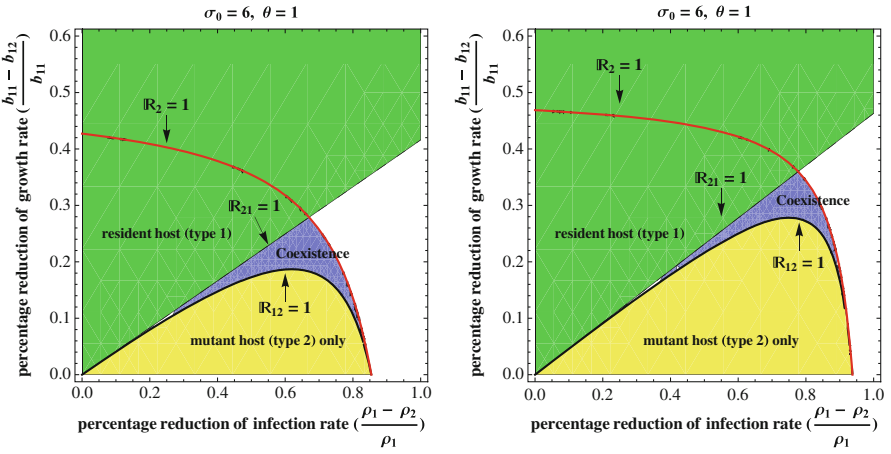

(a) $\sigma(a)$ is as shown in Figure 5(b). **(b)** $\sigma(a) > 0$ only for $10 < a \leq 30$.

Fig. 8 Similar to Fig. 7 but different age-dependent drug treatment programs are applied. Effects of two age-dependent treatment strategies, determined by the function $\sigma(a)$, are compared. The plot in **a** is for the case when $\sigma(a)$ has the form described in Fig. 5, whereas the plot in **b** is for the case in which only the age-group (10, 30] is targeted (i.e., $\sigma(a) \neq 0$ only for $10 < a \leq 30$). All other parameters have the same values as in Fig. 7. It demonstrates that the targeted treatment strategy makes it more likely for the mutant host type (parasite-resistant) to out-compete the resident type (parasite-susceptible)

example, a reduced infection rate (ρ_m) is associated with a lower birth rate (b_{1m}). That is, there is a functional relationship between b_{1m} and ρ_m:

$$b_{1m} = b_{1m}(\rho_m), \quad b'_{1m}(\rho_m) > 0.$$

We will also replace the subscripts 1 and 2 in $\Re_{21}$ by s and m, respectively, and have

$$\Re_{ms} = \Re_{21} = \frac{\frac{b_{1m}(\rho_m)}{b_{2m}+S_s^*+I_s^*}}{\mu_s + \rho_m c_s I_s^* \mathcal{R}_h},$$

where S_s^* and I_s^* are given in (16) and (17). Note that S_s^* and I_s^* are functions of ρ_s (the infection rate of snails of type s). Thus, $\Re_{ms} = \Re_{ms}(\rho_s, \rho_m)$ is a function of ρ_s and ρ_m.

From Result 4, the invasion condition for the mutant type host to invade the resident type host at the equilibrium $U_s^* = (S_s^*, I_s^*, 0, 0)$ is

$$\Re_{ms}(\rho_s, \rho_m) > 1. \tag{30}$$

For the mutant type to be more successful in the invasion, the quantity $\Re_{ms}$ (which can be considered as a measure of fitness for the mutant host) should be maximized. We will use $\Re_{ms}(\rho_s, \rho_m)$ to determine the evolutionary strategy. A strategy ρ^* is called an *evolutionarily singular strategy* if the fitness gradient satisfies the condition

$$\left.\frac{d\Re_{ms}}{d\rho_m}\right|_{\rho_m=\rho_s=\rho^*} = 0$$

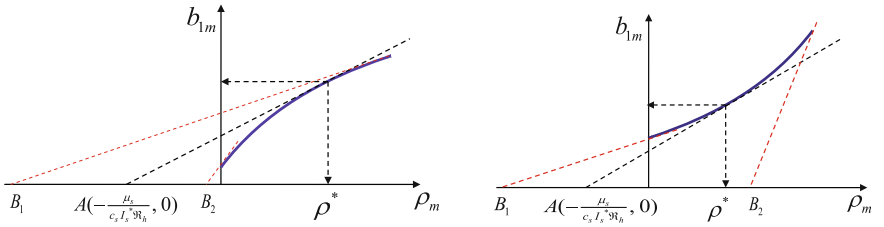

(a) Concave-down trade-off $b_{1m}(\rho_m)$ **(b)** Concave-up trade-off $b_{1m}(\rho_m)$

Fig. 9 Illustration of the graphical approach for identifying an evolutionarily singular strategy ρ^* for the trade-off function $b_{1m}(\rho_m)$ with two different properties. In **a** and **b**, the trade-off function $b_{1m}(\rho_m)$ is respectively concave-down and concave-up. B_1 and B_2 are the respective points where the *horizontal axis* intersects with the *tangent lines* of the trade-off curve passing through the two endpoints. An evolutionarily singular strategy can be determined by identifying a point ρ^* such that the tangent line of the curve $b_{1m}(\rho_m)$ at ρ^* passes through the point $A\left(-\frac{\mu_s}{c_s I_s^* \mathcal{R}_h}, 0\right)$

(see Geritz et al. 1997, 1998; Metz et al. 1996). An evolutionary singular strategy ρ^* is stable (i.e., ρ^* is an Evolutionary Stable Strategy or ESS) (Smith 1982) if

$$\Re_{ms}(\rho^*, \rho_m) < 1$$

for all $\rho_m \neq \rho^*$ in a neighborhood of ρ^* (Geritz et al. 1997, 1998; Metz et al. 1996). When ρ^* is an ESS, the host type using this strategy will not be invaded by any other host types.

We first discuss how an evolutionary singular strategy ρ^* can be determined. With some simplifications, we can rewrite the condition $d\Re_{ms}/d\rho_m = 0$ as

$$\frac{db_{1m}}{d\rho_m} = \frac{b_{1m}(\rho_m)}{\rho_m + \frac{\mu_s}{c_s I_s^* \mathcal{R}_h}}. \tag{31}$$

The condition (31) can be better understood by using a graphical interpretation as shown in Fig. 9. In this figure, the function $b_{1m} = b_{1m}(\rho_m)$ is plotted, which can be either concave-down and increasing (as shown in (a)) or concave-up and increasing (as shown in (b)). Notice that, if such a ρ^* exists, $\frac{db_{1m}(\rho^*)}{d\rho_m}$ is the slope of the line that passes through the two points $(\rho^*, b_{1m}(\rho^*))$ (which is on the curve $b_{1m}(\rho_m)$) and $A\left(-\frac{\mu_s}{c_s I_s^* \mathcal{R}_h}, 0\right)$ (which is on the ρ_m axis). Thus, an evolutionarily singular strategy can be determined by identifying a point ρ^* such that the tangent line of the curve $b_{1m}(\rho_m)$ at ρ^* passes through the point $A\left(-\frac{\mu_s}{c_s I_s^* \mathcal{R}_h}, 0\right)$.

From this geometric interpretation, we can see that not all functions $b_{1m}(\rho_m)$ will make it possible for ρ^* to exist, and that the existence of an evolutionarily singular strategy ρ^* will depend highly on the shape of the trade-off function. In addition, for ρ^* to exist, the point $A\left(-\frac{\mu_s}{c_s I_s^* \mathcal{R}_h}, 0\right)$ must lie between the points B_1 and B_2. Using the functional forms defined in the previous section, we consider two examples of $b_{1m}(\rho_m)$ which have significantly different shapes as shown in Fig. 11. This figure

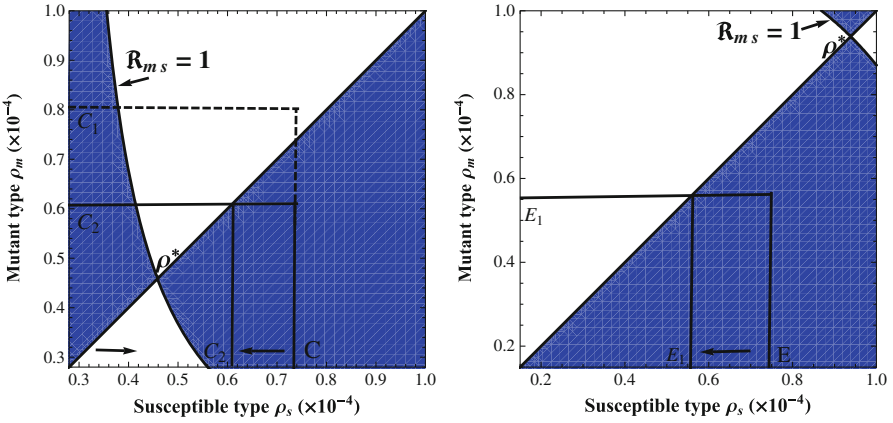

(a) The case of concave-down trade-off. **(b)** The case of concave-up trade-off.

Fig. 10 The figures in **a** and **b** illustrate the pairwise invasibility plots (PIP) for the cases when the trade-off function $b_{1m}(\rho_m)$ is concave-down and concave-up, respectively. The *horizontal axis* is the infection rate ρ_s of the susceptible (resident) type of snail host, and the *vertical axis* is the infection rate ρ_m of the resistant (mutant) type of snail host. In both plots, the invasion reproduction number satisfies the condition $\Re_{ms} < 1$ in the shaded region and $\Re_{ms} > 1$ in the unshaded region. All parameter values are the same as in Fig. 7

demonstrates how an evolutionarily singular strategy ρ^* can be determined for a given trade-off function $b_{1m}(\rho_m)$.

We now examine the stability and convergence of an evolutionarily singular strategy ρ^* using a pairwise-invasibility plot (PIP) (Geritz et al. 1997, 1998; Metz et al. 1996). To draw a PIP, we first need to choose parameters that can reflect the direction of evolution for the host. Here, we choose ρ_s and ρ_m to be the parameters, which represent the respective levels of parasite-resistance of the resident and mutant host types (see Fig. 10). Figure 10a, b is for the example a and example b, respectively, of the trade-off function $b_{1m}(\rho_m)$ shown in Fig. 11. In these PIPs, the fitness landscapes as experienced by a rare mutant correspond to the vertical lines where the resident trait value ρ_s is constant. Only mutants with trait values ρ_m for which $\Re_{ms} > 1$ are able to successfully invade. (note that $\Re_{ms}$ is a function of ρ_s and ρ_m). The two curves in each of these figures correspond to the threshold conditions $\Re_{ms} = 1$ (the decreasing curve) and $\Re_m = \Re_s$ (the diagonal line). The condition $\Re_{ms} > 1$ holds for points (ρ_s, ρ_m) in the shaded region, whereas the condition $\Re_{ms} < 1$ holds for points (ρ_s, ρ_m) in the unshaded region. The intersection of the two curves corresponds to an evolutionarily singular strategy ρ^* (Geritz et al. 1997, 1998).

An evolutionarily singular strategy ρ^* may or may not be an ESS. First, we look at Fig. 10a. Notice that for a given resident (susceptible) host with strategy C, if a mutant host uses a strategy C_1 with $C_1 > C$, then the point (C, C_1) falls in the unshaded region, in which case the mutant host cannot invade as $\Re_{ms} < 1$. However, if a mutant host uses a strategy C_2 with $C_2 < C$, then the point (C, C_2) falls into the shaded region, in which case the mutant host will be able to invade as $\Re_{ms} > 1$. In this case, the mutant type will replace the resident type and becomes the new resident type with the strategy C_2. If we repeat this process, it can be observed that as long as the strategy C_i is on the right-side of ρ^* (i.e., $C_i > \rho^*$), it will be replaced by a new

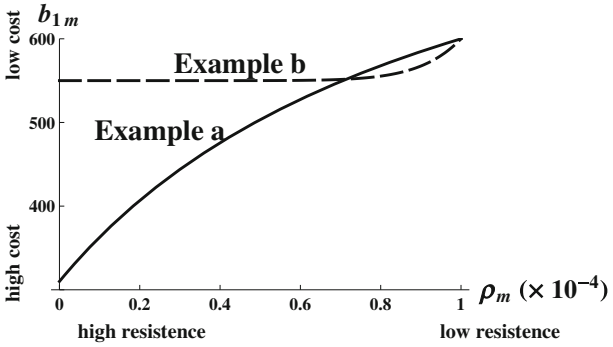

Fig. 11 Two examples of the cost function $b_{1m}(\rho_m)$. A higher infection rate ρ_m is associated with a lower parasite-resistance in the snail host, and a lower birth rate of snails is associated with a higher cost for parasite-resistance. *Examples a* and *b* represent the cases of the function $b_{1m}(\rho_m)$ being concave-down and concave-up, respectively. See the *text* for more explanations

strategy with a smaller value. Using a similar argument we know that if a strategy C_i is on the left-side of ρ^* (i.e., $C_i < \rho^*$), it will be replaced by a new strategy with a larger value. Thus, the parasite-resistance of the snail host will evolve towards ρ^* which acts as an evolutionary endpoint. Therefore, ρ^* is an ESS.

Next, we look at Fig. 10b. Using the similar argument as in Fig. 10a, we observe that for a given resident strategy E_i with $E_i < \rho^*$, a mutant with a strategy greater (smaller) than E_i cannot (can) invade the resident type. On the other hand, for a given resident strategy E_i with $E_i > \rho^*$, a mutant with a strategy greater (smaller) than E_i can (cannot) invade the resident type. Thus, the direction of evolution for parasite-resistance of the snail host will be away from ρ^*. In this case, ρ^* is unstable and unattainable, acting as an evolutionary repeller. This suggests that when there is variation in parasite-resistance, the evolutionary outcome could be the monomorphism of either the most or the least resistant snail type.

The trade-off examples a and b shown in Fig. 11 represent the cases of the function $b_{1m}(\rho_m)$ being concave-down and concave-up, respectively, which are used for generating Fig. 10. The lower bound for b_{1m} is set to be 310 which is low enough to guarantee a positive carrying capacity, i.e., $\frac{b_{1m}}{\mu_s} - b_{2m} > 0$, and the upper bound for b_{1m} is set to be 600 which is high enough to guarantee the existence of the two boundary equilibria U_1^* and U_2^*. The functional form used in Example a is $b_{1m}(\rho_m) = 890 - \frac{5.8\times10^{-2}}{\rho_m+10^{-4}}$, for which the cost of parasite-resistance increases more dramatically than the concave-up function in Example b, where $b_{1m}(\rho_m) = 550 + 0.5 \times 10^{42}\rho_m^{10}$.

The mathematical results in previous sections can be used to investigate how the ESS ρ^* may be influenced by the variation in virulence δ. Figure 12 shows that ρ^* increases with δ, which implies that higher parasite virulence favors less resistance (increased susceptibility) in snail hosts. This conclusion is consistent with Bowers et al. (1994) and Boots and Bowers (1999). Under these circumstances, when the parasite's virulence is higher, parasites kill infected snails more rapidly thereby lowering the infection probability. Consequently, there is lower pressure to avoid infection by paying reproductive costs associated with resistance. In this figure, we have used the concave-down function for $b_{1m}(\rho_m)$ as shown in Fig. 11a.

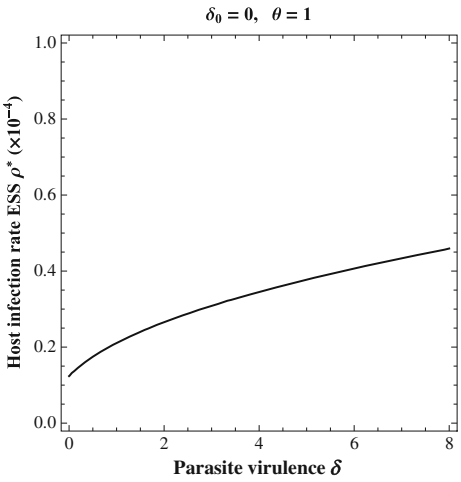

Fig. 12 Dependence of the evolutionarily stable strategy ρ^* on the parasite virulence δ to the snail host. This is for the case when drug-treatment in the human host is absent ($\sigma_0 = 0$) and there is no drug-resistance in the parasites ($\theta = 1$). All parameter values are the same as in Fig. 7

We can also look at the influence of drug-treatment in human hosts (σ) and associated drug-resistance of parasites (θ) in the ESS ρ^*. We need to point out that when considering drug-treatment in human hosts, it is more realistic to take into account human migration among villages which likely influences water-contact rates with various water bodies. However, this requires the use of a metapopulation approach (i.e., models that include a collection of sub-populations with connections between these sub-populations), which dramatically increases the complexity of the model. For simplicity, our model here assumes that human and snail populations are stable in time and space. We can examine the influence of drug-treatment of humans in the ESS ρ^* by using the two reproduction rates $\gamma(\theta)$ given in (28) and (29). Figure 13a shows that the ESS ρ^* increases with σ_0 (the background rate of drug-treatment). That is, higher infection rates (more susceptible snail type) will be selected when drug-treatment level is high. This occurs because the probability of infection will be lower when drug-treatment rate is high; and thus, the pressure to avoid infection is low and it is more beneficial for snail hosts to remain susceptible. For fixed σ_0, a higher cost for drug-resistance favors higher infection rate (more susceptible snail type). This is because (under same conditions) the density of miracidia is lower in the case of "high cost" (28) than in the case of "low cost" (29).

The dependence of the ESS ρ^* on the level of drug-resistance θ is not as simple (see Fig. 13b), as it can also be affected by the shape of the function $\gamma(\theta)$. If we consider the case of "high cost" for drug-resistance (given in (28)), the solid curve in Fig. 13b shows that intermediate values of drug-resistance level θ are associated with lower infection rates in snails (i.e., higher parasite-resistance in snails). However, as θ increases further, the ESS ρ^* increases with θ which implies that lower levels of parasite-resistance will be favored. To understand this nonmonotonic response, we need to look at the effect of drug-resistance θ on the whole system. As a higher level of drug-resistance θ reduces the effectiveness of drug-treatment σ, a higher density of parasites may be expected. On the other hand, because of the cost for drug-resistance, the reproduction rate $\gamma(\theta)$ will be decreased, which may lower the parasite density.

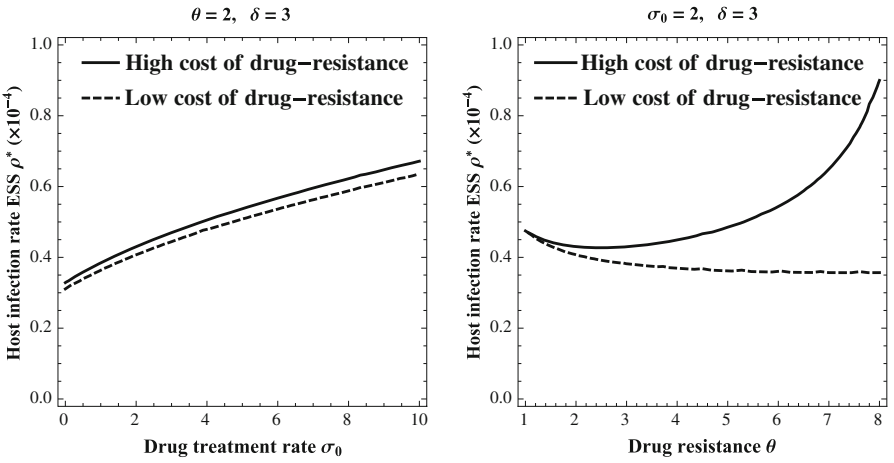

(a) ρ^* vs. the level of drug treatment. **(b)** ρ^* vs. the level of drug-resistance.

Fig. 13 **a** Dependence of the evolutionarily stable ρ^* on the background drug treatment rate σ_0 for given levels of drug-resistance (θ) and virulence in the snail hosts (δ). **b** Dependence of the evolutionarily stable ρ^* on the drug-resistance level θ for given levels of drug-treatment (σ_0) and virulence (δ). The *solid curve* is for the case when the function $\gamma(\theta)$ in (28) is used, and the *dotted curve* is for the case when the function $\gamma(\theta)$ in (29) is used

Depending on the shapes of trade-offs (27) and (28) (note that $f(\sigma)$ is concave-up and $\gamma(\theta)$ is linear with respect to θ), the change due to the reduced drug-resistance is more dramatic when the drug-resistance level θ is lower. Thus, in the case of "high cost" for drug-resistance (and for fixed drug-treatment rate σ_0), for low drug-resistance values (smaller θ) the resistant type of snail host is favored; whereas for high drug-resistance values (larger θ) the susceptible type of snail host is favored. In the case of "low cost" for drug-resistance, the dotted curve in Fig. 13b shows that the ESS ρ^* decreases with θ. Thus, higher drug-resistance levels select for lower infection rates in the snails, leading to a more resistant type of snail host.

5 Discussion

In this paper, we employed a model for the snail–schistosome–human system to study the transmission dynamics of the system and its implications for evolutionary outcomes of the host–parasite interactions. Evolutionary dynamics of host–parasite interactions are of great interest to biologists and epidemiologists. Many mathematical models have been used to study the outcomes of these interactions, but most of these models are for parasites with direct life cycles. The model we studied here is for parasites with an indirect life cycle (such as schistosome). These models are usually more complex and their analyses are more challenging mathematically. Nevertheless, these models are important to consider as they may provide novel insights into the underlying processes that impact the evolutionary outcomes of host–parasite interactions, as demonstrated in this study.

The model studied in this paper incorporates both the definitive human host and two types of intermediate snail hosts. Age-structure of human hosts is also considered

to reflect the age-dependent transmission rates, which makes it possible to study age-targeted drug treatment rates as well as associated drug resistance in the parasites. We analyzed the mathematical properties of the model in terms of stabilities of steady states and possible appearance of stable periodic solutions, and calculated the basic reproductive numbers $\Re_i$ of the parasites associated with the snail hosts of type i ($i = 1, 2$). Furthermore we derived the invasion reproduction numbers $\Re_{ji}$ for the snail host of type j when type i is at an endemic equilibrium E_i^* ($1 \le i \ne j \le 2$), which are used to explore the evolutionary outcomes of the host–parasite system.

Our results show that the reproduction numbers $\Re_i$ and $\Re_{ji}$ provide threshold conditions that determine the parasite-resistance of snail hosts, infection levels of parasites, and evolutionary outcomes for both parasites and hosts. By constructing various bifurcation diagrams involving relevant model parameters, we were able to examine the roles of several biological factors (e.g., trade-offs between parasite-resistance and reproduction of the snail hosts, trade-offs between virulence and reproduction of parasites, and trade-offs between drug-resistance and regeneration of parasites) in influencing the evolutionary outcomes of this host–parasite system. Using the approach of evolutionary stable strategy (ESS) and the method of pairwise invasibility plots (PIP), we demonstrated how ESS may depend on specific functional forms under various model assumptions, such as the cost function $b_{1m}(\rho_m)$ for the growth rate of snail hosts due to parasite-resistance. We presented examples which illustrate that the stability and convergence of an evolutionary singular strategy may depend on the specific functional forms of $b_{1m}(\rho_m)$. This kind of conclusion is of great interests to evolutionary biologists, and it has led to the development of three distinct geometric approaches that allow for the evolutionary study of models while keeping the role of geometry of the trade-offs explicit (see Bowers et al. 2005; de Mazancourt and Dieckmann 2004; Rueffler et al. 2004 for more details).

Most of the assumptions used in our analyses were based on either experimental results or observations from natural systems. Our findings suggest that model results can be very sensitive to model assumptions in some cases, and much less sensitive in others. Our results have also allowed us to draw interesting conclusions in terms of competitive outcomes between host types. For example, we found that, under the assumed trade-off between the cost of parasite-resistance in snails (ρ_i) and the snail reproductive rate (b_{1i}), the likelihood of host polymorphism increases as the degree of difference between the two snail host types increases, suggesting that the cost of parasite-resistance may contribute to the maintenance of resistance polymorphism in this system. This mechanism may help to explain the occurrence of such patterns in a number of host species from *Daphnia* (Duncan and Little 2007) to *Drosophila* (Kraaijeveld and Godfray 1997) to snails (Webster and Woolhouse 1999).

We have also obtained other conclusions from the model analyses. For example, when parasite virulence is high (i.e., the parasite-induced death rate in the snail host is large), the parasite-susceptible snail type may exclude a parasite-resistant type for the given trade-off functions. This result may seem counter-intuitive, as higher parasite virulence is often predicted to favor host investment in resistance. However, in this case, reductions in host survival may inadvertently lead to this result, by reducing transmission probabilities. Therefore, hosts may be more fit by *not* investing in resistance due to the low probability of actually becoming infected by a virulent parasite.

In addition, we found that different drug-treatment rates of human hosts ($\sigma(a)$) and the trade-off functions for drug-resistance may interact to alter the ESS. When we used the particular functional form of $\gamma(\theta)$, a more susceptible snail host type was favored when the drug-treatment rate of humans is high. This has significant biological and epidemiological ramifications, as attempts to reduce infection at one stage of the parasite life cycle (humans) may, in fact lead to enhanced susceptibility of hosts at another stage of the life cycle.

This modeling study focuses on assessing the roles that host life-history, parasite transmission, virulence, and drug therapy play in shaping populations of an indirectly transmitted parasite and its hosts. The models used in this work include several simplifying assumptions. One example is that the sex ratio of adult worms within human hosts is assumed to be 1:1 although the ratios in nature population are usually male-biased (2:1). The role of schistosome mating structure in host–parasite interactions has been considered previously using mathematical models (see, for example, Xu et al. 2005). Nonetheless, even with these simplifications, results from this research can provide important insights into the factors responsible for parasite transmission and the emergence of drug resistance in the field.

We remark that the model considered in this paper includes only a single parasite strain, and we have focused mainly on the evolutionary outcomes of the intermediate hosts in terms of the their resistance to infection. An extension of this model can be considered in which both multiple types of snail hosts and multiple parasite strains can be included explicitly. Then questions concerning co-evolutionary dynamics of hosts and parasites can be studied. Such models will certainly be more complicated and more challenging to analyze mathematically. Even for the simplified model (4), only partial analysis have been carried out and more detailed examination is still needed to identify the roles played by other factors. For example, when we considered the effect of drug treatment of human hosts, we fixed the age-distributions of infection rate $\beta(a)$ and the age-dependent treatment $\sigma(a)$, and varied only the constant σ_0. The structure of model (4) actually allows us to explore the impact of various age-distributions of transmission and drug treatment ($\beta(a)$ and $\sigma(a)$) on the evolutionary outcomes of the host–parasite interactions. Figure 8 illustrates a such example. Additional results on the influence of age structure will be presented elsewhere.

Acknowledgments We thank the reviewers for very helpful comments that improved the manuscript. This research is partially supported by NSF grants DMS-0719697 and DMS-0719783.

Appendix

In this appendix, we provide an outline of the derivation for the age-structured equations for $n(t, a)$ and $p(t, a)$ in (1) as well as proofs for some of the results stated in the main text.

Derivation of the equations for $n(t, a)$ and $p(t, a)$ in (1)

The definitions of $n(t, a)$ and $p(t, a)$ are adopted from Hadeler (1984) and Hadeler and Dietz (1983), and the derivation presented here also follows their approach. The

difference is that they do not consider intermediate hosts; and thus, the infection rate of humans is proportional to the total density of parasites. Here, we assume that the infection rate of humans is proportional to the total density of cercariae C.

Let $H(t,a,x)$ denote the number of human hosts of age a at time t, carrying x adult parasites. Assume that the rate at which a human host acquires one parasite is proportional to $C(t)$ with (host) age-dependent proportionality constant $\beta(a)$. Then the number of parasites within a host of age a can increase from $x-1$ to x by acquiring a new parasite at the rate $\beta(a)C$, and decrease from $x+1$ to x due to either the natural death of parasites at the per-capita rate μ_p or being killed by drug treatment at the rate $f(\sigma(a))$. Here $\sigma(a)$ represents the age-targeted drug treatment rate for the human hosts. Assume also that all parasites within a host will die if the host dies, which occurs at the per-capita rate $\mu_h(a)$ (note that the mortality of human hosts due to parasites is ignored in this paper). Then, we have the following infinite system of partial differential equations for $H(t,a,x)$:

$$\begin{aligned}\left(\frac{\partial}{\partial t}+\frac{\partial}{\partial a}\right)H(t,a,x)&=\beta(a)CH(t,a,x-1)+\left(\mu_p+f(\sigma)\right)(x+1)H(t,a,x+1)\\&\quad-\left[\beta(a)C+\mu_h+\left(\mu_p+f(\sigma)\right)x\right]H(t,a,x),\quad \text{for}\quad x\geq 1,\end{aligned}\tag{32}$$

$$\left(\frac{\partial}{\partial t}+\frac{\partial}{\partial a}\right)H(t,a,0)=\left(\mu_p+f(\sigma)\right)H(t,a,1)-\left(\beta(a)C+\mu_h\right)H(t,a,0),$$
$$\text{for } x=0.$$

Let $n(t,a)$ denote the total number of human hosts of age a at time t, and let $p(t,a)$ denote the total number of parasites carried by human hosts of age a at time t. Then

$$n(t,a)=\sum_{x=0}^{\infty}H(t,a,x),\quad p(t,a)=\sum_{x=1}^{\infty}xH(t,a,x).$$

Adding equations in (32) accordingly we have

$$\left(\frac{\partial}{\partial t}+\frac{\partial}{\partial a}\right)n(t,a)=-\mu_h(a)n(t,a),$$
$$\left(\frac{\partial}{\partial t}+\frac{\partial}{\partial a}\right)p(t,a)=\beta(a)n(t,a)C(t)-\left(\mu_h(a)+\mu_p+f(\sigma(a))\right)p(t,a),$$

which are the same equations as in (1).

Proof of Result 2

For ease of presentation we introduce the notation

$$\mu_k=\mu_s+\delta_k,\quad k=1,2.\tag{33}$$

Linearizing the system (11) at an equilibrium point $(\bar{S}_k, \bar{I}_k)$ we get the following characteristic equation

$$\det\begin{pmatrix} \frac{b_{1k}(b_{2k}+\bar{I}_k)}{(b_{2k}+\bar{S}_k+\bar{I}_k)^2} - \rho_k c_k \bar{I}_k \mathcal{R}_h - \mu_s - \lambda & -\frac{b_{1k}\bar{S}_k}{(b_{2k}+\bar{S}_k+\bar{I}_k)^2} - \rho_k c_k \bar{S}_k \hat{R}_h(\lambda) \\ \rho_k c_k \bar{I}_k \mathcal{R}_h & \rho_k c_k \bar{S}_k \hat{R}_h(\lambda) - \mu_k - \lambda \end{pmatrix} = 0, \tag{34}$$

where $\hat{R}_h(\lambda)$ denotes the Laplace transform of $R_h(\tau)$, i.e.,

$$\hat{R}_h(\lambda) = \int_0^\infty R_h(\tau) e^{-\lambda\tau} d\tau, \tag{35}$$

and λ is an eigenvalue.

At $E_{k0} = (S_{k0}, 0)$, the characteristic equation (34) simplifies to

$$\left(\lambda + \frac{b_{1k} S_{k0}}{(b_{2k} + S_{k0})^2}\right)\left(\lambda - \rho_k c_k S_{k0} \hat{R}_h(\lambda) + \mu_k\right) = 0, \tag{36}$$

which has one negative eigenvalue $\lambda = -\frac{b_{1k} S_{k0}}{(b_{2k}+S_{k0})^2}$ with other eigenvalues being given by the equation

$$f(\lambda) = \lambda - \rho_k c_k S_{k0} \hat{R}_h(\lambda) + \mu_k = 0.$$

Notice that $\frac{d}{d\lambda}\hat{R}_h < 0$, which implies that $f(\lambda)$ is an increasing function. Notice also that

$$f(0) = -\rho_k \left(\frac{b_{1k}}{\mu_s} - b_{2k}\right) c_k \mathcal{R}_h + \mu_k = \mu_k(1 - \Re_k).$$

It follows that $f(\lambda)$ has no nonnegative real roots if $\Re_k < 1$ and one positive real root if $\Re_k > 1$. Thus, E_{k0} is unstable if $\Re_k > 1$.

For the case of $\Re_k < 1$, we need to show that $f(\lambda)$ does not have complex roots with nonnegative real part. Suppose that $\lambda = x + yi$ is a complex root of $f(\lambda)$ with $x \geq 0$. Then the equation $f(\lambda) = 0$ becomes

$$f(x + yi) = x + yi - \rho_k \left(\frac{b_{1k}}{\mu_s} - b_{2k}\right) c_k \int_0^\infty R_h(a) e^{-(x+yi)a} da + \mu_k = 0.$$

Thus, the real part of $f(x + yi)$ must be zero, i.e.

$$Re(f(x + yi)) = x - \rho_k \left(\frac{b_{1k}}{\mu_s} - b_{2k}\right) c_k \int_0^\infty R_h(a) e^{-xa} \cos ya da + \mu_k = 0. \tag{37}$$

On the other hand, notice that $Re(f(x+yi)) \geq f(x)$ and that $f(x) \geq f(0) > 0$. Thus, $Re(f(x+yi)) > 0$, which contradicts (37). It follows that E_{k0} is locally asymptotically stable when $\Re_k < 1$. This finishes the proof of part (a).

To prove part (b), i.e., the stability of E_k^*, we notice that the characteristic equation at E_k^* is

$$\det \begin{pmatrix} -\dfrac{b_{1k}S_k^*}{(b_{2k}+S_k^*+I_k^*)^2} - \lambda & -\dfrac{b_{1k}S_k^*}{(b_{2k}+S_k^*+I_k^*)^2} - \rho_k c_k S_k^* \hat{R}_h(\lambda) \\ \rho_k M_k^* & \rho_k c_k S_k^* \hat{R}_h(\lambda) - \mu_k - \lambda \end{pmatrix} = 0, \quad (38)$$

where $\hat{R}_h(\lambda)$ is given in (35) and

$$M_k^* = c_k I_k^* \mathcal{R}_h.$$

In the characteristic equation (38), we have used the fact that at E_k^* (see (17)),

$$\frac{b_{1k}}{b_{2k}+S_k^*+I_k^*} - \rho_k c_k I_k^* \mathcal{R}_h - \mu_s = 0.$$

Rewrite the characteristic equation (38) as

$$G(\lambda) = 0, \quad (39)$$

where

$$\begin{aligned} G(\lambda) = &\left(\lambda + \frac{b_{1k}S_k^*}{(b_{2k}+S_k^*+I_k^*)^2}\right)\left(\lambda - \rho_k c_k S_k^* \hat{R}_h(\lambda) + \mu_k\right) \\ &+ \rho_k M_k^* \left(\frac{b_{1k}S_k^*}{(b_{2k}+S_k^*+I_k^*)^2} + \rho_k c_k S_k^* \hat{R}_h(\lambda)\right). \end{aligned} \quad (40)$$

For ease of the proof, we consider a variation of the the equation $G(\lambda) = 0$. Notice that the function $G(\lambda)$ can be written as

$$\begin{aligned} G(\lambda) = &\left(\lambda + \frac{b_{1k}S_k^*}{\left(b_{2k}+S_k^*+I_k^*\right)^2} - \frac{b_{1k}}{b_{2k}+S_k^*+I_k^*} + \rho_k M_k^* + \mu_s\right)\left(\lambda - \rho_k S_k^* c_k \hat{R}_h + \mu_k\right) \\ &+ \rho_k M_k^* \left(\frac{b_{1k}S_k^*}{(b_{2k}+S_k^*+I_k^*)^2} + \rho_k S_k^* c_k \hat{R}_h\right) \\ = &\left(\lambda + \frac{b_{1k}S_k^*}{\left(b_{2k}+S_k^*+I_k^*\right)^2} - \frac{b_{1k}}{b_{2k}+S_k^*+I_k^*} + \mu_s\right)(\lambda + \mu_k) \\ &- \rho_k S_k^* c_k \hat{R}_h \left(\lambda + \frac{b_{1k}S_k^*}{\left(b_{2k}+S_k^*+I_k^*\right)^2} - \frac{b_{1k}}{b_{2k}+S_k^*+I_k^*} + \mu_s\right) + \rho_k M_k^* (\lambda + \mu_k) \end{aligned}$$

$$+\rho_k M_k^* \frac{b_{1k} S_k^*}{\left(b_{2k} + S_k^* + I_k^*\right)^2}$$
$$= (\lambda + z^*)(\lambda + \mu_k) - \rho_k S_k^* c_k \hat{R}_h(\lambda + z^*) + \rho_k M_k^* (\lambda + \mu_k) + \frac{b_{1k} \rho_k M_k^* S_k^*}{\left(b_{2k} + S_k^* + I_k^*\right)^2},$$

where

$$z^* = \frac{b_{1k} S_k^*}{\left(b_{2k} + S_k^* + I_k^*\right)^2} - \frac{b_{1k}}{b_{2k} + S_k^* + I_k^*} + \mu_s.$$

Straightforward calculations yield that $G(-z^*) \neq 0$, i.e., $\lambda = -z^*$ is not a root of $G(\lambda)$. Thus, we can divide both sides of the equation $G(\lambda) = 0$ by $\lambda + z^*$ and obtain the following equation which is equivalent to $G(\lambda) = 0$:

$$H(\lambda) = \lambda + \mu_k - \rho_k S_k^* c_k \hat{R}_h + \rho_k M_k^* \frac{\lambda + \mu_k}{\lambda + z^*} + \frac{b_{1k} \rho_k M_k^* S_k^*}{(b_{2k} + S_k^* + I_k^*)^2} \frac{1}{\lambda + z^*} = 0.$$

We first show that for $z^* > 0$, $H(\lambda)$ does not have roots (either real or complex) with positive real part. Suppose that $\lambda = x + yi$ is a root of $H(\lambda)$ with $x > 0$. Then, from the fact that $\rho_k c_k S_k^* \mathcal{R}_h - \mu_k = 0$ (see (16)) we know that the real part of $H(x + yi)$ satisfies

$$\begin{aligned} Re(H(x+yi)) &= x + \mu_k - \rho_k c_k S_k^* \int_0^\infty e^{-xa} \cos(ya) R_h(a) da \\ &\quad + \rho_k M_k^* \frac{(x+\mu_k)(x+z^*) + y^2}{(x+z^*)^2 + y^2} + \frac{b_{1k} \rho_k M_k^* S_k^*}{(b_{2k} + S_k^* + I_k^*)^2} \frac{x + z^*}{(x+z^*)^2 + y^2} \\ &> x + \mu_k - \rho_k c_k S_k^* \int_0^\infty e^{-xa} \cos(ya) R_h(a) da \\ &\geq x + \mu_k - \rho_k c_k S_k^* \mathcal{R}_h \\ &= x > 0. \end{aligned}$$

However, $Re(H(x+yi)) = 0$. This contradiction implies that $H(\lambda)$, and hence $G(\lambda)$, has no roots with positive real part when $z^* > 0$.

The following relations show that $\lambda = 0$ is not a root of $G(\lambda)$:

$$G(0) = \frac{b_{1k} S_k^*}{\left(b_{2k} + S_k^* + I_k^*\right)^2} \left(-\rho_k S_k^* c_k \mathcal{R}_h + \mu_k\right) + \rho_k M_k^* \left(\frac{b_{1k} S_k^*}{\left(b_{2k} + S_k^* + I_k^*\right)^2} + \rho_k S_k^* c_k \mathcal{R}_h \right)$$

$$
\begin{aligned}
&> \frac{b_{1k}S_k^*}{\left(b_{2k}+S_k^*+I_k^*\right)^2}\left(-\rho_k S_k^* c_k \mathcal{R}_h + \mu_k\right) \\
&= \frac{b_{1k}S_k^*}{\left(b_{2k}+S_k^*+I_k^*\right)^2}\left(\mu_k - \rho_k c_k \mathcal{R}_h \frac{\mu_k}{\rho_k c_k \mathcal{R}_h}\right) \\
&= 0.
\end{aligned}
$$

Therefore, we have shown that $z^* > 0$ is a sufficient condition for the stability of E_k^*.

Although it is not clear from the expression of z^* whether or not z^* may change its sign for realistic values of the model parameters, our numerical calculations show that both $z^* > 0$ and $z^* < 0$ are possible. Under the condition $z^* > 0$, if we choose b_{1k} as a bifurcation parameter (with all other parameters fixed), then we can numerically determine a threshold value $\tilde{b}_{1k}$ such that

$$z^* > 0 \quad \text{if and only if} \quad b_{1k} < \tilde{b}_{1k}.$$

Thus, $b_{1k} < \tilde{b}_{1k}$ provides a sufficient condition for E_k^* to be locally asymptotically stable.

When $b_{1k} > \tilde{b}_{1k}$ or equivalently $z^* < 0$, it is possible that the characteristic equation $G(\lambda)$ may have complex roots with opposite signs. In fact, our numerical calculations show that there exists a critical point $b_{1k} = b_{1k}^*$ such that for b_{1k} near b_{1k}^*, E_k^* is stable when $b_{1k} < b_{1k}^*$ and unstable when $b_{1k} > b_{1k}^*$, in which case a stable periodic solution exists (see Fig. 2).

The proof of Result 2 is completed.

Proof of Result 3

Let μ_k $(k = 1, 2)$ be as defined in (33). The characteristic equation at the equilibrium U_{10} is

$$
\begin{aligned}
F_1(\lambda) = &\left(\lambda + \frac{b_{11}S_{10}}{(b_{21}+S_{10})^2}\right)(\lambda+\mu_2)\left(\lambda - \rho_1 S_{10} c_1 \hat{R}_h + \mu_1\right) \\
&\times \left(\lambda - \frac{b_{12}}{b_{22}+S_{10}} + \mu_s\right) = 0,
\end{aligned}
$$

where $S_{10} = b_{11}/\mu_s - b_{12}$. It is easy to check that the condition (19) implies that the eigenvalue $\frac{b_{12}}{b_{22}+S_{10}} - \mu_s < 0$. From the proof of the stability of E_1^* in Sect. 3.1 we know that the function $\lambda - \rho_1 S_{10} c_1 \hat{R}_h + \mu_1$ has all roots with negative real part when $\Re_1 < 1$ and at least one positive root when $\Re_1 > 1$. It follows that U_{10} is locally asymptotically stable when $\Re_1 < 1$ and unstable when $\Re_1 > 1$.

Similarly, the characteristic equation at the equilibrium U_{02} is

$$F_2(\lambda) = \left(\lambda + \frac{b_{12}S_{02}}{(b_{22}+S_{02})^2}\right)(\lambda+\mu_1)\left(\lambda - \rho_2 S_{02} c_2 \hat{R}_h + \mu_2\right) \times \left(\lambda - \frac{b_{11}}{b_{21}+S_{02}} + \mu_s\right) = 0,$$

where $S_{02} = b_{12}/\mu_s - b_{22}$. From the condition (19) we can verify that the eigenvalue $\frac{b_{11}}{b_{21}+S_{02}} - \mu_s > 0$. Thus, U_{02} is unstable.

This finishes the proof of Result 3.

Proof of Result 4

Let μ_k $(k = 1, 2)$ be as defined in (33). The proof for the existence of U_1^* follows from that for E_1^* of the reduced system (3.1). For the stability of U_1^*, notice that the characteristic equation at U_1^* is

$$\det\begin{pmatrix} J_1 & * \\ 0 & J_4 \end{pmatrix} = 0,$$

where

$$J_1 = \begin{pmatrix} -\frac{b_{11}S_1^*}{(b_{21}+S_1^*+I_1^*)^2} - \lambda & -\frac{b_{11}S_1^*}{(b_{21}+S_1^*+I_1^*)^2} - \rho_1 c_1 \hat{R}_h S_1^* \\ \rho_1 c_1 I_1^* \mathcal{R}_h & \rho_1 c_1 \hat{R}_h S_1^* - \mu_1 - \lambda \end{pmatrix},$$

$$J_4 = \begin{pmatrix} \frac{b_{12}}{b_{22}+S_1^*+I_1^*} - \rho_2 c_1 I_1^* \mathcal{R}_h - \mu_s - \lambda & 0 \\ \rho_2 c_1 I_1^* \mathcal{R}_h & -\mu_2 - \lambda \end{pmatrix}.$$

From the proof for the stability of E_1^* we know that, under the conditions $b_{11} < \tilde{b}_{11}$ and $\Re_1 > 1$, all solutions of the equation $\det(J_1) = 0$ have negative real parts. Thus, U_1^* is stable if all solutions of $\det(J_4) = 0$ have negative real parts. This is true if

$$\frac{b_{12}}{b_{22}+S_1^*+I_1^*} - \rho_2 c_1 I_1^* \mathcal{R}_h - \mu_s < 0, \tag{41}$$

which is equivalent to $\Re_{21} < 1$. U_1^* is unstable if the inequality (41) is reversed, which is equivalent to $\Re_{21} > 1$.

The proof of Result 4 is completed.

References

Anderson RM, May RM (1978) Regulation and stability of host-parasite population interactions. I. Regulatory processes. J Anim Ecol 47:219–247

Anderson RM, May RM (1982) Coevolution of hosts and parasites. Parasitology 85:411–426
Anderson RM, May RM (1991) Infectious diseases of humans. Dynamics and control. Oxford university Press, Oxford
Beck K, Keener JP, Ricciardi P (1984) The effects of epidemics on genetic evolution. J Math Biol 19:79–94
Boots M, Bowers RG (1999) Three mechanisms of host resistance to microparasites-avoidance, recovery and tolerance—show different evolutionary dynamics. J Theor Biol 201:13–23
Boots M, Haraguchi Y (1999) The evolution of costly resistance in host-parasite systems. Am Nat 153(4):359–370
Bowers RG (1999) A baseline model for the apparent competition between many host types: the evolution of host resistance to microparasites. J Theor Biol 200:65–67
Bowers RG, Turner J (1997) Community structure and the interplay between interspecific infection and competition. J Theor Biol 187:95–109
Bowers RG, Boots M, Begon M (1994) Life-history trade-offs and the evolution of pathogen resistance: competition between host strain. Proc R Soc Lond B 257:247–253
Bowers RG, Hoyle A, White A, Boots M (2005) The geometric theory of adaptive evolution: trade-off and invasion plots. J Theor Biol 233:363–377
CDC—Schistosomiasis biology (2011). http://www.cdc.gov/parasites/schistosomiasis/biology.html. Accessed July 2011
CDC—Schistosomiasis fact sheet (2011). http://www.cdc.gov/parasites/schistosomiasis/epi.html. Accessed July 2011
Chan MS, Guyatt HL, Bundy DA, Booth M, Fulford AJ, Medley GF (1995) The development of an age structured model for schistosomiasis transmission dynamics and control and its validation for *Schistosoma mansoni*. Epidemiol Infect 115:325–344
Chitsulo L, Engels D, Montresor A, Savioli L (2000) The global status of schistosomiasis and its control. Acta Trop 77:41–51
Cioli D (2000) Praziquantel: is there real resistance and are there alternatives? Curr Opin Infect Dis 13: 659
Davies CM, Webster JP, Woolhouse MEJ (2001) Trade-offs in the evolution of virulence in an indirectly transmitted macroparasite. Proc R Coc Lond B 268:251–257
de Mazancourt C, Dieckmann U (2004) Trade-off geometries and frequency-dependent selection. Am Nat 164(6):765–778
Diekmann O, Heesterbeek JAP (2000) Mathematical epidemiology of infectious diseases: model building, analysis and interpretation. Wiley, New York
Dobson AP (1988) The population biology of parasite-induced changes in host behavior. Q Rev Biol 63:139–165
Dobson AP, Keymer AE (1985) Life history models. In: Crompton DWT, Nickol BThe biology of the Acanthocephala. Cambridge University Press, Cambridge, pp 347–384
Duncan AB, Little TJ (2007) Parasite-driven genetic change in a natural population of *Daphnia*. Evolution 61(4):796–803
Fallon PG, Mubarak JS, Fookes RE, Niang M, Butterworth AE, Sturrock RF, Doenhoff MJ (1997) *Schistosoma mansoni*: maturation rate and drug susceptibility of different geographic isolates. Exp Parasitol 86:29–36
Feng Z, Eppert A, Milner FA, Minchella DJ (2004) Estimation of parameters governing the transmission dynamics of Schistosomes. Appl Math Lett 17:105
Frank SA (1992) A kin selection model for the evolution of virulence. Proc R Soc Lond B 250:195–197
Gerard C, Theron A (1997) Age/size- and time-specific effects of *Schistosoma mansoni* on energy allocation patterns of its snail host *Biomphalaria glabrata*. Oecologia 112:447–452
Geritz SAH, Metz JAJ, Kisdi E, Meszena G (1997) The dynamics of adaptation and evolutionary branching. Phys Rev Lett 78:2024–2027
Geritz SAH, van der Meijden E, Metz JAJ (1998) Evolutionarily singular strategies and the adaptive growth and branching of the evolutionary tree. Evol Ecol 12:35–57
Gower CM, Webster JP (2004) Fitness of indirectly transmitted pathogens: restraint and constraint. Evolution 58:544–553
Gower CM, Webster JP (2005) Intraspecific competition and the evolution of virulence in a parasitic trematode. Evolution 59:544–553

Hadeler KP (1984) An integral equation for helminthic infections: stability of the noninfected population. In: Lakeshmikantham V (ed) Trends in theoretical and practical nonlinear differential equations. Lecture notes in pure and applied mathematics, vol 90. Marcel Dekker

Hadeler KP, Dietz K (1983) Nonlinear hyperbolic partial differential equations for the dynamics of parasite populations. Comput Math Appl 9(3):415–430

Hoyle A, Bowers RG (2008) Can possible evolutionary outcomes be determined directly from the population dynamics? Theor Popul Biol 74:311–323

Ismail M, Botros S, Metwally A, William S et al (1999) Resistance to Praziquantel: direct evidence from *Schistosoma mansoni* isolated from Egyptian villagers. Am J Trop Med Hyg 60(6):932–935

Kraaijeveld AR, Godfray HCJ (1997) Trade-off between parasitoid resistance and larval competitive ability in *Drosophila melanogaster*. Nature 389:278–280

Massara CL, Peixoto SV, Barros HS, Enk MJ, Carvalho OS, Schall V (2004) Factors associated with *Schistosomiasis Mansoni* in a population from the municipality of Jaboticatubas, State of Minas Gerais, Brazil. Mem Inst Oswaldo Cruz, Rio de Janeiro 99(Suppl I):127–134

May RM, Anderson RM (1983) Epidemiology and genetics in the coevolution of parasites and hosts. Proc R Soc Lond B 219:281–313

May RM, Nowak MA (1995) Coinfection and the evolution of virulence. Proc R Soc Lond B 261:209–215

Metz JAJ, Nisbet RM, Geritz SAH (1992) How should we define 'fitness' for general ecological scenarios? Trends Ecol Evol 7:198–202

Metz JAJ, Geritz SAH, Meszena G, Jacobs FJA, Heerwaarden JS (1996) Adaptive dynamics: a geometrical study of the consequences of nearly faithful reproduction. In: van Strien SJ, Verduyn Lunel SM (eds) Stochastic and spatial structures of dynamical systems. North Holland, Amsterdam, pp 183–231

Meuleman EA (1972) Host-parasite interrelationships between the freshwater pulmonate *Biomphalaria pfeifferi* and the trematode *Schistosoma mansoni*. Neth J Zool 22:355–427

Miller MR, White A, Boots M (2005) The evolution of host resistance: tolerance and control as distinct strategies. J Theor Biol 236:198–207

Minchella DJ (1985) Host life-history variation in response to parasitism. Parasitology 90:205–216

Minchella DJ, Loverde PT (1981) A cost of increased reproductive effort in the snail *Biomphalaria glabrata*. Am Nat 118:876–881

Nowak MA, May RM (1994) Superinfection and the evolution of parasite virulence. Proc R Soc Lond B 255:81–89

Pan CT (1965) Studies on the host-parasite relationship between *Schistosoma mansoni* and the Snail *Australorbis glabratus*. Am J Trop Med Hyg 14(6):931–976

Rueffler C, van Dooren TJM, Metz JAJ (2004) Adaptive walks on changing landscapes: Levins' approach extended. Theor Popul Biol 65:165–178

Rugierri E, Schreiber SJ (2005) The dynamics of the Schoener-Polis-Holt model of intra-guild predation. Math Biosci Eng 2(2):279–288

Sandland GJ, Minchella DJ (2003a) Costs of immune defense: an enigma wrapped in an environmental cloak? Trends Parasitol 19:571–574

Sandland GJ, Minchella DJ (2003b) Effects of diet and *Echinostoma revolutum* infection on energy allocation patterns in juvenile *Lymnaea elodes* snails. Oecologia 134:479–486

Sandland GJ, Minchella DJ (2004) Life-history plasticity in hosts exposed to differing resources and parasitism. Can J Zool 82:1672–1677

Smith JM (1982) Evolution and the theory of games. Cambridge University Press, Cambridge

Sorensen RE, Minchella DJ (2001) Snail-trematode life history interactions: past trend and future directions. Parasitology 123:S3–S18

Sturrock RF (2001) Schistosomiasis epidemiology and control: how did we get here and where should be go? Mem Inst Oswaldo Cruz, Rio de Janeiro 96(Suppl):17–27

Webster JP, Woolhouse MEJ (1999) Cost of resistance: relationship between reduced fertility and increased resistance in a snail–schistosome host–parasite system. Proc R Soc B: Biol Sci 266:391–396

Xu D, Curtis J, Feng Z, Minchella DJ (2005) On the role of schistosome mating structure in the maintenance of drug resistant strains. Bull Math Biol 67(6):1207–1226

Zhang P, Feng Z, Milner FA (2007a) A schistosomiasis model with an age-structure in human hosts and its application to treatment strategies. Math Biosci 205(1):83–107

Zhang P, Sandland GJ, Feng Z, Xu D, Minchella DJ (2007b) Evolutionary implications for interactions between multiple strains of host and parasite. J Theor Biol 248(2):225–240